



UvA-DARE (Digital Academic Repository)

Near-ads₂ spectroscopy

Classifying the spectrum of operators and interactions in $N = 2$ 4d supergravity

Castro, A.; Verheijden, E.

DOI

[10.3390/universe7120475](https://doi.org/10.3390/universe7120475)

Publication date

2021

Document Version

Final published version

Published in

Universe

License

CC BY

[Link to publication](#)

Citation for published version (APA):

Castro, A., & Verheijden, E. (2021). Near-ads₂ spectroscopy: Classifying the spectrum of operators and interactions in $N = 2$ 4d supergravity. *Universe*, 7(12), [475].
<https://doi.org/10.3390/universe7120475>

General rights



It is not permitted to download or to forward/distribute the text or part of it without the consent of the author(s) and/or copyright holder(s), other than for strictly personal, individual use, unless the work is under an open content license (like Creative Commons).

Disclaimer/Complaints regulations

If you believe that digital publication of certain material infringes any of your rights or (privacy) interests, please let the Library know, stating your reasons. In case of a legitimate complaint, the Library will make the material inaccessible and/or remove it from the website. Please Ask the Library: <https://uba.uva.nl/en/contact>, or a letter to: Library of the University of Amsterdam, Secretariat, Singel 425, 1012 WP Amsterdam, The Netherlands. You will be contacted as soon as possible.

Article

Near-AdS₂ Spectroscopy: Classifying the Spectrum of Operators and Interactions in $\mathcal{N} = 2$ 4D Supergravity

Alejandra Castro  and Evita Verheijden Delta Institute for Theoretical Physics-Institute of Physics, University of Amsterdam,
1098 XH Amsterdam, The Netherlands

* Correspondence: a.castro@uva.nl (A.C.); e.m.h.verheijden@uva.nl (E.V.)

Abstract: We describe holographic properties of near-AdS₂ spacetimes that arise within spherically symmetric configurations of $\mathcal{N} = 2$ 4D $U(1)^4$ supergravity for both gauged and ungauged theories. These theories pose a rich space of AdS₂ × S² backgrounds, and their responses in the near-AdS₂ region are not universal. In particular, we show that the spectrum of operators is dual to the matter fields, and their cubic interactions are sensitive to properties of the background and the theory it is embedded in. The properties that have the most striking effect are whether the background is supersymmetric or not and if the theory is gauged or ungauged. Interesting effects are due to the appearance of operators with $\Delta < 2$, which depending on the background, can lead to, for instance, instabilities or extremal correlators. The resulting differences will have an imprint on the quantum nature of the microstates of near-extremal black holes, reflecting that not all extremal black holes respond equally when kicked away from extremality.

Keywords: black holes; supergravity; AdS/CFT correspondence

Citation: Castro, A.; Verheijden, E. Near-AdS₂ Spectroscopy: Classifying the Spectrum of Operators and Interactions in $\mathcal{N} = 2$ 4D Supergravity. *Universe* **2021**, *7*, 475. <https://doi.org/10.3390/universe7120475>

Academic Editor: Norma G. Sanchez

Received: 25 October 2021
Accepted: 1 December 2021
Published: 4 December 2021

Publisher's Note: MDPI stays neutral with regard to jurisdictional claims in published maps and institutional affiliations.



Copyright: © 2021 by the authors. Licensee MDPI, Basel, Switzerland. This article is an open access article distributed under the terms and conditions of the Creative Commons Attribution (CC BY) license (<https://creativecommons.org/licenses/by/4.0/>).

1. Introduction

Recent years have seen great progress in understanding the quantum properties of black holes in the context of the AdS/CFT correspondence. While the universal nature of the Bekenstein–Hawking area-law reflects that there should be a commonality in the statistical origin of their entropy, this might not be the case for a refined description. Our goal here is to underscore aspects of black holes that are not universal, despite their shared semi-classical features. In particular, we will bring to light concise holographic data that are sensitive to the surrounding theory that fosters the black hole and to the interplay of the theory content with properties of the background.

Our analysis is embedded in the developments coined as the near-AdS₂/near-CFT₁ correspondence [1,2]. This instance of holography describes deformations away from an idealised AdS₂ geometry, which are relevant to construct a holographic description of the near-horizon region of near-extremal black holes. One of the most prominent results of near-AdS₂/near-CFT₁ was to show that the leading gravitational backreaction, which defines near-AdS₂, is universally encoded in two-dimensional Jackiw–Teitelboim (JT) gravity [3,4]. This is the commonality that is nowadays used to decode quantum properties of black holes. Building on these developments, here we wish to further decode what other degrees of freedom appear as one backreacts the geometry and how these degrees of freedom interact with the JT sector. In particular, we will report on the spectrum of fluctuations in the near-horizon region, which we translate to the spectrum of operators in the CFT₁, and cubic interactions among these fluctuations.

We will focus on some of the simplest scenarios of near-AdS₂ that one might expect to lead to a UV-complete description in string theory: backgrounds that arise as solutions to a four-dimensional supergravity theory and connect to suitable near-extremal black holes therein. With regard to these theories, we will study solutions of four-dimensional $\mathcal{N} = 2$ supergravity, covering both gauged and ungauged cases, which we describe in

more detail below. The overarching feature of these theories is that they contain four $U(1)$ gauge fields and six real scalar fields (with three of them being axions). We will consider configurations in four dimensions that respect spherical symmetry, where the extremal near-horizon region is precisely $\text{AdS}_2 \times S^2$. This makes it possible to build an effective two-dimensional description by integrating out the 2-sphere and to tie our results to the features of JT gravity in a simple manner.

The strategy presented here is as follows. We will start with an $\text{AdS}_2 \times S^2$ background that solves the equations of four-dimensional $\mathcal{N} = 2$ supergravity. We will first proceed to study linearised perturbations around this background that preserve spherical symmetry. From here, we will single out the JT sector, which encodes the features of near- AdS_2 ; we will also organize the remaining perturbations according to their scaling dimension and interpret them as dual operators. The second step is to characterise the cubic interactions among these operators and the JT sector and quantify the leading correction of their two-point functions due to these interactions. This closely follows the analysis in [5] and is also mentioned in [2,6].

There are two important features that have the biggest imprint on our analysis. The first one is the “background”: our starting point is an AdS_2 solution, characterised by a set of electric and magnetic charges, and the six scalar fields are controlled by the attractor mechanism [7–14]. As we consider different AdS_2 backgrounds in the gauged and ungauged theory, the most important feature of each background is if the solution preserves supersymmetry, i.e., if the extremal black hole is BPS¹ or non-BPS. The spectrum of operators is highly sensitive to this feature. In the ungauged theory, the non-BPS black holes will contain marginal operators, which is a direct consequence of having a flat direction in the attractor mechanism [15]; these operators will lead to extremal three-point correlators that are pathological. On the other hand, the operators in the BPS branch in the ungauged theory all have conformal dimension $\Delta = 2$, placing them on a similar footing to the JT sector, in agreement with the nAttractor proposed in [16]. For the gauged theory, non-BPS AdS_2 backgrounds have modes that violate the Breitenlohner–Freedman (BF) stability bound in AdS_2 [17], which signals an instability along the lines of [18]. BPS black holes, in contrast, do not exhibit these instabilities, nor do they contain marginal operators.

The second crucial feature comes from the “surrounding”: the theory within which the solution is embedded. Here it is important to account for all scalar fields present in the truncation, and if the theory is gauged or ungauged. The presence of the cosmological constant in the gauged theory, in comparison to the ungauged theory, tends to lower the conformal dimensions of the operators. For non-BPS backgrounds, this leads to the BF instabilities aforementioned, which are unique to the gauged theory. For BPS backgrounds, the gauged theory will contain relevant operators and irrelevant ones that have $1 < \Delta < 3/2$; the presence of this matter content indicates that the Schwarzian mode of JT gravity is not supposed to be the dominant effect (see [2]). The behaviour of the interactions is also rather different: for the backgrounds in the gauged theory, the cubic couplings allow for both positive and negative signs, depending on the conformal dimensions of the fields, while in the ungauged theory they have definite signs.

Although we are restricting the discussion here to $\text{AdS}_2 \times S^2$ near-horizon backgrounds, relevant for static dyonic black holes, we will only discuss certain solutions. Their properties and relation to extremal black holes are the following.

- **BPS branch, ungauged theory:** our analysis covers the most general dyonic solution with four magnetic and four electric charges. We will follow conventions of [19], where the corresponding black hole solution is described in detail. A more recent discussion on extremal dyonic black holes can be found in [20].
- **Non-BPS branch, ungauged theory:** we will cover a large class of non-BPS solutions, but with certain limitations, since the attractor equations generically admit non-linear solutions. The corresponding black hole solution will again follow [19], and prior works of interest here include [11,21,22] and references therein.

- **Magnetic, BPS, gauged theory:** these are backgrounds that carry four magnetic charges and preserve supersymmetry. The corresponding black holes were first constructed in [23], and accounting for the Bekenstein–Hawking entropy in AdS₄/CFT₃ was first performed in [24].
- **Magnetic, non-BPS, gauged theory:** we focus on magnetic solutions that smoothly interpolate from the gauged to the ungauged theory and hence are not supersymmetric within AdS₄. These black holes date back to [25], and our conventions follow [26].
- **Dyonic, non-BPS, gauged theory:** to illustrate the effects of dyonic backgrounds in the gauged theory, we consider a simple case with only one electric and one magnetic charge. The corresponding black hole is in [26].

As reflected by this list, static black holes embedded in AdS₄ are notoriously more difficult to construct and analyse, which is the reason that our examples in the gauged theory are more limited. Other solutions that we are not considering here, but are worth investigating, are the most general dyonic static BPS black holes in AdS₄ gauged supergravity [27,28]—with their statistical interpretation via the dual CFT performed in [29]. There are also many other non-BPS solutions in the gauged theory, see e.g. [26,30], and one could also consider near-horizon geometries of the form AdS₂ × Σ_g, with Σ_g a two-dimensional Riemann surface of genus g , which we will not do here.

In the context of near-AdS₂/near-CFT₁ and its ties to near-extremal black holes, the Reissner–Nördstrom solution was an important lamppost in these developments. Some of the original references are [31,32], which also include dyonic cases. An important generalisation here is to embed these solutions carefully within a supergravity theory and quantify the effects that the background and surrounding have on the dictionary that dictates properties of the near-CFT₁.² These properties, the spectrum of operators and interactions, show to us how building a statistical interpretation of the different cases explored here is already highly non-trivial, and it will require a more intricate dual description—in comparison to the SYK-like models studied in, for instance [35–39].

This paper is organised as follows. We start in Section 2 by introducing the four-dimensional $\mathcal{N} = 2$ supergravity theory and its field content, and the dimensional reduction to AdS₂ × S². In Section 3, we describe general aspects of the near-AdS₂ analysis. We discuss the AdS₂ background and the attractor mechanism and study linearised perturbations of the dilaton, scalar fields, and the metric around this background. We single out the JT sector and discuss the cubic interactions of the matter fields with this sector. We quantify the correction of these interactions on the two-point functions of the matter fields. In Section 4, we evaluate these expressions explicitly for the ungauged theory. We classify the solutions according to them being BPS or non-BPS and contrast the responses of the near-AdS₂ region and the corrections to the two-point functions in both branches. As mentioned above, we find that fluctuations around BPS backgrounds comply with the attractor mechanism, but for non-BPS solutions, we find a marginal operator corresponding to a flat direction in the attractor mechanism. For non-BPS backgrounds, we find non-vanishing cubic couplings for certain extremal correlators and discuss the repercussions of this pathology. In Section 5, we consider some special cases in the gauged theory: purely magnetic solutions, both BPS and non-BPS, and a dyonic non-BPS solution with a single charge. We classify the non-universal features at the level of the spectrum of operators and the interactions. We end in Section 6 with a careful discussion of our results and discuss future directions. We also included four appendices: in Appendix A, we gather some basic conventions and notation; in Appendix B, we collect explicit formulas necessary to integrate out the field strengths for our U(1)⁴ supergravity theory and the attractor solutions for this theory (for general charges and purely magnetic solutions). In Appendix C, we give explicit expressions for the linearised equations and interactions for purely magnetic (BPS and non-BPS) backgrounds. Finally, in Appendix D, we explain how to set up the extremal limit for both BPS and non-BPS black hole solutions and give a numerical example illustrating the appearance of a flat direction in the linear response.

2. Two-Dimensional Effective Field Theory Description

2.1. $\mathcal{N} = 2 U(1)^4$ Gauged Supergravity

Our analysis is centred around bosonic solutions to $\mathcal{N} = 2 U(1)^4$ gauged supergravity in four dimensions. This theory can be viewed as an Abelian truncation to the Cartan subgroup $U(1)^4$ of $\mathcal{N} = 8 SO(8)$ gauged supergravity [25]. Our conventions follow those in [26], which we quickly summarise here. Note that these conventions differ in very minor ways relative to e.g., [25,40], where the definitions of the scalar fields are slightly different relative to the description here.

The basic ingredients of this supergravity theory are the following. The bosonic fields are the metric $g_{\mu\nu}^{(4)}$, six real scalar fields, and four gauge fields. The scalar fields are split into three dilatons, φ_i and three axions, χ_i with $i = 1, 2, 3$; the gauge fields are labelled as A^I with $I = 1, 2, 3, 4$. Because we are in four dimensions, there are several formulations of the action since the gauge fields can be dualised; the dual gauge field will be denoted as \tilde{A}_I , and the corresponding field strengths are

$$F^I = dA^I, \quad \tilde{F}_I = d\tilde{A}_I. \tag{1}$$

To describe the dynamical aspects of the theory, we will use here the dual formulation as described in [26], where the action is given by

$$I_{4D} = \frac{1}{16\pi G_4} \int d^4x \sqrt{-g^{(4)}} \mathcal{L}_{4D}, \tag{2}$$

and

$$\begin{aligned} \mathcal{L}_{4D} = & R^{(4)} - \frac{1}{2} \sum_{i=1}^3 \left((\partial\varphi_i)^2 + e^{2\varphi_i} (\partial\chi_i)^2 \right) + g^2 \sum_{i=1}^3 \left(2 \cosh \varphi_i + \chi_i^2 e^{\varphi_i} \right) \\ & - \frac{1}{4} e^{-\varphi_1} \left(e^{\varphi_2 + \varphi_3} (\mathcal{F}^1)^2 + e^{\varphi_2 - \varphi_3} (\tilde{\mathcal{F}}_2)^2 + e^{-\varphi_2 + \varphi_3} (\tilde{\mathcal{F}}_3)^2 + e^{-\varphi_2 - \varphi_3} (\mathcal{F}^4)^2 \right) \\ & - \frac{1}{4} \chi_1 \epsilon^{\mu\nu\alpha\beta} \left(F_{\mu\nu}^1 F_{\alpha\beta}^4 + \tilde{F}_{2\mu\nu} \tilde{F}_{3\alpha\beta} \right). \end{aligned} \tag{3}$$

Here g is a real gauge-coupling constant, which effectively acts as a negative cosmological constant; setting $g = 0$ gives rise to the STU model in ungauged supergravity. The calligraphic field strengths are related to those in (1) via

$$\begin{aligned} \mathcal{F}^1 &= F^1 + \chi_3 \tilde{F}_2 + \chi_2 \tilde{F}_3 - \chi_2 \chi_3 F^4, \\ \tilde{\mathcal{F}}_2 &= \tilde{F}_2 - \chi_2 F^4, \\ \tilde{\mathcal{F}}_3 &= \tilde{F}_3 - \chi_3 F^4, \\ \mathcal{F}^4 &= F^4, \end{aligned} \tag{4}$$

where two of our gauge fields (\tilde{F}_2, \tilde{F}_3) are treated in terms of their duals. It will be useful to rewrite the terms involving field strengths in (3) as

$$\begin{aligned} \mathcal{L}_{4D} = & R^{(4)} - \frac{1}{2} \sum_{i=1}^3 \left((\partial\varphi_i)^2 + e^{2\varphi_i} (\partial\chi_i)^2 \right) + g^2 \sum_{i=1}^3 \left(2 \cosh \varphi_i + \chi_i^2 e^{\varphi_i} \right) \\ & - \frac{1}{4} k_{IJ} \mathbf{F}^I_{\mu\nu} \mathbf{F}^{J\mu\nu} + \frac{1}{4} h_{IJ} \epsilon^{\mu\nu\alpha\beta} \mathbf{F}^I_{\mu\nu} \mathbf{F}^J_{\alpha\beta}. \end{aligned} \tag{5}$$

We have introduced some notation to reflect that we are in a mixed situation where some fields are dualised: in our case of interest, we have

$$\mathbf{F}^I \equiv (F^1, \tilde{F}_2, \tilde{F}_3, F^4). \tag{6}$$

Expressions for the matrices k_{IJ} and h_{IJ} in terms of φ_i and χ_i are written in Appendix B.

2.2. Dimensional Reduction

In the following, we will perform the dimensional reduction of bosonic solutions to $\mathcal{N} = 2 U(1)^4$ gauged supergravity that preserves spherical symmetry. The outcome of this subsection is an effective two-dimensional action that fully captures the dynamics of four-dimensional spherically symmetric backgrounds. There are several references that perform a very similar analysis to ours. We will mostly follow [16] for the treatment of the gauge fields, and the metric will be treated as in e.g., [32].

We will write backgrounds that preserve spherical symmetry as

$$ds^4 = \frac{1}{\Phi(x)} g_{ab} dx^a dx^b + \Phi^2(x) (d\theta^2 + \sin^2 \theta d\phi^2). \tag{7}$$

Here x^a are two-dimensional coordinates, with $a, b = 0, 1$, and g_{ab} is the two-dimensional metric.³ The scalar $\Phi(x)$ is the radius of the 2-sphere, and it is also introduced as a conformal factor for g_{ab} . The relative powers of Φ in (7) are selected such that the four-dimensional Ricci scalar is related to its two-dimensional counterpart as

$$R^{(4)} = \Phi R^{(2)} + \frac{2}{\Phi^2} - \frac{3}{\Phi} g^{ab} \nabla_a (\Phi \nabla_b \Phi). \tag{8}$$

The last term here will correspond to a total derivative when replaced back in (2), and hence there will be no explicit kinetic terms for $\Phi(x)$ in our final answer; $\Phi(x)$ will be referred to as the dilaton. In the following, we will discuss the remaining matter fields—four field strengths and six scalars—and write the resulting two-dimensional theory obtained by placing (2) on the background (7). We are also only focusing on the so-called *s*-wave sector of the theory, which implies that the matter fields will respect the isometries of the 2-sphere made manifest in (7). For the six scalars (φ_i, χ_i) , this means that we will assume they only depend on x^a .

Next, we focus on the field strengths supported by the background (7). Because of the spherical symmetry, and since the spacetime is a direct product, one can solve in full generality for the field strengths that respect this structure, i.e., one can integrate them out. To be concrete, the general two-form that conforms with the symmetries of (7) will be of the form

$$F^I = (\dots) \epsilon_{ab} dx^a \wedge dx^b - P^I \sin \theta d\theta \wedge d\phi, \tag{9}$$

and

$$\tilde{F}_I = (\dots) \epsilon_{ab} dx^a \wedge dx^b + Q_I \sin \theta d\theta \wedge d\phi. \tag{10}$$

Here ϵ_{ab} is the epsilon tensor for g_{ab} . Note that $\sin \theta d\theta \wedge d\phi$ is the volume form in S^2 , so this just reflects that F^I and F_I are linear combinations of the volume (top) forms on g_{ab} and S^2 . P^I and Q_I are constants that correspond to magnetic and electric charges: notice that F^I carries the magnetic charge in the angular components, while \tilde{F}_I carries the electric charge in the angular components.⁴ The (\dots) will be polynomials of the scalars Φ, φ_i and χ_i to be determined by imposing the equations of motion for the field strengths. This is what we want to write explicitly in the following.

The equation of motion from varying with respect to F^I is given by

$$\nabla_\mu (k_{IJ} F^{J\mu\nu} - h_{IJ} \epsilon^{\mu\nu\alpha\beta} F^J_{\alpha\beta}) = 0, \tag{11}$$

where we are adopting the notation in (5). Since we are assuming that $\varphi_i = \varphi_i(x)$ and $\chi_i = \chi_i(x)$, the angular components of this equation are automatically satisfied by (9) and (10). The components along x^a have a simple solution given by

$$\Phi^3 k_{IJ} F^J_{ab} - 2h_{IJ} P^J \epsilon_{ab} = Q_I \epsilon_{ab}, \tag{12}$$

where we have made use of (7) and cast the solution in terms of the two-dimensional metric g_{ab} . It is straightforward to invert this equation since both k_{IJ} and h_{IJ} have an inverse, and the explicit solution is given in (A14). We also introduced the bold notation for the charges

$$\mathbf{Q}_I \equiv (Q_1, P^2, P^3, Q_4), \quad \mathbf{P}^I \equiv (P^1, -Q_2, -Q_3, P^4). \tag{13}$$

With this notation, we can simply rewrite (9) and (10) as

$$\mathbf{F}^I = \frac{1}{2} \mathbf{F}_{ab}^I dx^a \wedge dx^b - \mathbf{P}^I \sin \theta d\theta \wedge d\phi, \tag{14}$$

with \mathbf{F}_{ab}^I determined by (12).

Given that it is very simple to solve for \mathbf{F}^I , in the process of constructing our effective two-dimensional theory, we will integrate them out; i.e., we want to trade \mathbf{F}^I for $(\mathbf{P}^I, \mathbf{Q}_I)$. For the components of \mathbf{F}^I along the 2-sphere, this is a simple replacement of (14) in the action. For \mathbf{F}_{ab}^I , this requires performing a Legendre transform to consistently trade it for \mathbf{Q}_I in the action and comply with the equations of motion; for a more detailed discussion, see, for example, ref. [16]. The steps are the following: start with the contribution to the action from the second line of (5), and replace (7) and (14), which gives

$$\begin{aligned} & \frac{1}{16\pi G_4} \int d^4x \sqrt{-g^{(4)}} \left(-\frac{1}{4} k_{IJ} \mathbf{F}_{\mu\nu}^I \mathbf{F}^{J\mu\nu} + \frac{1}{4} h_{IJ} \epsilon^{\mu\nu\alpha\beta} \mathbf{F}_{\mu\nu}^I \mathbf{F}_{\alpha\beta}^J \right) \\ & = \frac{1}{4G_4} \int d^2x \sqrt{-g^{(2)}} \Phi^3 \left(-\frac{1}{4} k_{IJ} (\mathbf{F}_{ab}^I \mathbf{F}^{Jab} + \frac{2}{\Phi^6} \mathbf{P}^I \mathbf{P}^J) - \frac{h_{IJ}}{\Phi^3} \epsilon^{ab} \mathbf{F}_{ab}^I \mathbf{P}^J \right). \end{aligned} \tag{15}$$

The second step is the Legendre transform, which amounts to adding to the action the term

$$- \frac{1}{8G_4} \int d^2x \sqrt{-g^{(2)}} \epsilon^{ab} \mathbf{Q}_I \mathbf{F}_{ab}^I. \tag{16}$$

After adding this term to (15) it is consistent to replace \mathbf{F}_{ab}^I with $(\mathbf{P}^I, \mathbf{Q}_I)$ via (12).

Finally, incorporating all of our ingredients, we can write the effective two-dimensional theory. Using (7), (8), (15), and (16), our two-dimensional action and Lagrangian are

$$I_{2D} = \frac{1}{4G_4} \int d^2x \sqrt{-g^{(2)}} \mathcal{L}_{2D}, \tag{17}$$

and

$$\begin{aligned} \mathcal{L}_{2D} &= \Phi^2 R^{(2)} + \frac{2}{\Phi} + g^2 \Phi \sum_{i=1}^3 \left(2 \cosh \varphi_i + \chi_i^2 e^{\varphi_i} \right) \\ & - \frac{\Phi^2}{2} \sum_{i=1}^3 \left((\partial_a \varphi_i) (\partial^a \varphi_i) + e^{2\varphi_i} (\partial^a \chi_i) (\partial_a \chi_i) \right) - \frac{1}{2\Phi^3} V(\mathbf{P}, \mathbf{Q}). \end{aligned} \tag{18}$$

Here, $V(\mathbf{P}, \mathbf{Q})$ is a scalar potential encoding the magnetic and electric charges⁵

$$V(\mathbf{P}, \mathbf{Q}) \equiv (\mathbf{P}^I \ \mathbf{Q}_I) \begin{pmatrix} k_{IJ} + 4h_{IK}(k^{-1})^{KL}h_{LJ} & -2h_{IK}(k^{-1})^{KJ} \\ -2(k^{-1})^{IK}h_{KJ} & (k^{-1})^{IJ} \end{pmatrix} \begin{pmatrix} \mathbf{P}^J \\ \mathbf{Q}_J \end{pmatrix}. \tag{19}$$

This Lagrangian is a consistent truncation for the s-wave sector of $U(1)^4$ gauged supergravity when compactified on S^2 , and it will be the main object that we will use in the coming section.

Lastly, it will be useful to record the equations of motion associated to (18). Varying with respect to the dilaton gives

$$\begin{aligned} \Phi R^{(2)} &= \frac{1}{\Phi^2} - \frac{g^2}{2} \sum_{i=1}^3 \left(2 \cosh \varphi_i + \chi_i^2 e^{\varphi_i} \right) - \frac{3}{4\Phi^4} V \\ &+ \frac{\Phi}{2} \sum_{i=1}^3 \left((\partial_a \varphi_i)(\partial^a \varphi_i) + e^{2\varphi_i} (\partial^a \chi_i)(\partial_a \chi_i) \right). \end{aligned} \tag{20}$$

The equations of motion from varying the scalars φ_i and χ_i are, respectively,

$$\begin{aligned} \nabla_a \left(\Phi^2 \nabla^a \varphi_i \right) - \Phi^2 e^{2\varphi_i} g^{ab} \partial_a \chi_i \partial_b \chi_i + g^2 \Phi (2 \sinh \varphi_i + \chi_i^2 e^{\varphi_i}) - \frac{1}{2\Phi^3} \partial_{\varphi_i} V &= 0, \\ \nabla_a \left(\Phi^2 e^{2\varphi_i} \nabla^a \chi_i \right) + 2g^2 \Phi \chi_i e^{\varphi_i} - \frac{1}{2\Phi^3} \partial_{\chi_i} V &= 0. \end{aligned} \tag{21}$$

Finally, the equation obtained by variation with respect to the two-dimensional metric g_{ab} is

$$\begin{aligned} (\nabla_a \nabla_b - g_{ab} \square) \Phi^2 + \frac{\Phi}{2} \sum_{i=1}^3 \left((\partial_a \varphi_i)(\partial_b \varphi_i) + e^{2\varphi_i} (\partial_a \chi_i)(\partial_b \chi_i) \right) \\ + \left[\frac{1}{\Phi} + \frac{g^2}{2} \Phi \sum_{i=1}^3 \left(2 \cosh \varphi_i + \chi_i^2 e^{\varphi_i} \right) - \frac{1}{4\Phi^3} V - \frac{\Phi^2}{4} \sum_{i=1}^3 \left((\partial \varphi_i)^2 + e^{2\varphi_i} (\partial \chi_i)^2 \right) \right] g_{ab} &= 0. \end{aligned} \tag{22}$$

In the next section, we will use these equations of motion to study linear perturbations.

3. General Aspects of the Near-AdS₂ Analysis

In this section, we describe general aspects of the holographic dictionary for near-AdS₂ solutions. The aim is to study corners of this dictionary that are sensitive to the surrounding matter content. We will start by constructing the AdS₂ backgrounds, which describe the near-horizon geometry of extremal black holes in supergravity. Second, we will discuss the linearised perturbations around the AdS₂ solution. This will allow us to identify the JT sector—which encodes the deviations away from extremality that are characteristic of near-AdS₂—and the matter degrees of freedom due to the embedding in supergravity. Third, we will describe the interactions of the matter fields with the JT sector.

3.1. AdS₂ Background: IR Fixed Point

The AdS₂ backgrounds are characterised by having all of the scalars in play equal to a constant: this is the characteristic feature of an attractor mechanism. We will refer to these AdS₂ solutions interchangeably as either the attractor solution or the IR fixed point. Starting with the scalars of our theory in (18), we will write

$$\varphi_i = \bar{\varphi}_i, \quad \chi_i = \bar{\chi}_i, \quad \Phi = \Phi_0, \tag{23}$$

where the right-hand sides are constant values. Inserting this into the dilaton equation (20) gives

$$2\Phi_0 R^{(2)} - \frac{2}{\Phi_0^2} + g^2 \sum_i (2 \cosh \bar{\varphi}_i + \bar{\chi}_i^2 e^{\bar{\varphi}_i}) + \frac{3}{2\Phi_0^4} \bar{V} = 0, \tag{24}$$

where \bar{V} indicates that we should evaluate the matrix entries at the fixed point, i.e., $\bar{V} \equiv V(\mathbf{P}, \mathbf{Q})|_{\varphi_i=\bar{\varphi}_i, \chi_i=\bar{\chi}_i}$. This equation makes it very clear that at the IR fixed point, the two-dimensional metric is locally AdS₂. To compensate for the odd factors in (7), we will set

$$g_{ab} = \Phi_0 \bar{g}_{ab}, \tag{25}$$

where \bar{g}_{ab} is a locally AdS₂ spacetime with radius ℓ_2 . Combining (24) with the Einstein Equation (22), we obtain

$$\begin{aligned} \frac{1}{\ell_2^2} + \frac{1}{\Phi_0^2} &= \frac{1}{2\Phi_0^4} \bar{V}, \\ \frac{1}{\ell_2^2} - \frac{1}{\Phi_0^2} &= g^2 \sum_i (2 \cosh \bar{\varphi}_i + \bar{\chi}_i^2 e^{\bar{\varphi}_i}). \end{aligned} \tag{26}$$

Using (23), the equations for the scalars in (21) are

$$g^2 (2 \sinh \bar{\varphi}_i + \bar{\chi}_i^2 e^{\bar{\varphi}_i}) - \frac{1}{2\Phi_0^4} \partial_{\bar{\varphi}_i} \bar{V} = 0, \tag{27}$$

and

$$2g^2 \bar{\chi}_i e^{\bar{\varphi}_i} - \frac{1}{2\Phi_0^4} \partial_{\bar{\chi}_i} \bar{V} = 0. \tag{28}$$

where the derivatives of the potential are simply

$$\partial_{\bar{\varphi}_i} \bar{V} \equiv \left. \frac{\partial V}{\partial \varphi_i} \right|_{\varphi_i = \bar{\varphi}_i, \chi_i = \bar{\chi}_i}, \tag{29}$$

and similar for $\partial_{\bar{\chi}_i} \bar{V}$ and multiple derivatives of the potential.

In Appendix B.1 we write explicitly how the attractor Equations (27)–(28) depend on $(\mathbf{P}^I, \mathbf{Q}_I)$, which illustrates more clearly how $\bar{\varphi}_i$ and $\bar{\chi}_i$ depend on the charges. In Section 4, we discuss the solutions of the ungauged case, and in Section 5, we solve these equations explicitly for special cases in the gauged theory.

It is important to stress that until this point, we have not imposed supersymmetry on the background AdS₂ solution: we are only demanding that we have an extremal solution. As we explore explicit cases in gauged ($g^2 > 0$) and ungauged supergravity ($g = 0$), we will describe how imposing BPS conditions on the background affects our subsequent analysis of the near-AdS₂ dynamics.

3.2. Linear Analysis: Spectrum of Operators and JT Sector

The first entry in the holographic analysis we will decode are the linear fluctuations around the AdS₂ background, and we will identify the degrees of freedom. Following similar steps as in [5,41], we define

$$\begin{aligned} \Phi &= \Phi_0 + \mathcal{Y}, \\ \varphi_i &= \bar{\varphi}_i + \boldsymbol{\varphi}_i, \\ \chi_i &= \bar{\chi}_i + \boldsymbol{\chi}_i, \\ g_{ab} &= \Phi_0 \bar{g}_{ab} + h_{ab}, \end{aligned} \tag{30}$$

where $(\Phi_0, \bar{\varphi}_i, \bar{\chi}_i, \bar{g}_{ab})$ define the zeroth-order AdS₂ background of Section 3.1, and $(\mathcal{Y}, \boldsymbol{\varphi}_i, \boldsymbol{\chi}_i, h_{ab})$ are the corresponding fluctuations.

At the linear level in the fluctuations, using (30) in the equations of motion gives the following results. Upon using the zeroth-order equations for the background, at leading order, the Einstein Equation (22) gives

$$(\bar{\nabla}_a \bar{\nabla}_b - \bar{g}_{ab} \bar{\square}) \mathcal{Y} + \frac{1}{\ell_2^2} \bar{g}_{ab} \mathcal{Y} = 0. \tag{31}$$

As expected, this defines \mathcal{Y} to comply with the equation of motion characteristic of JT gravity. The trace of this equation implies that

$$\bar{\square} \mathcal{Y} = \frac{2}{\ell_2^2} \mathcal{Y}, \tag{32}$$

which identifies \mathcal{Y} as an operator of conformal dimension $\Delta_{\mathcal{Y}} = 2$. Next, the linearised equations derived from (21) are given by

$$0 = \square \varphi_i + \left(g^2 (2 \cosh \bar{\varphi}_i + \bar{\chi}_i^2 e^{\bar{\varphi}_i}) - \frac{1}{\ell_2^2} - \frac{1}{\Phi_0^2} \right) \varphi_i + \frac{4g^2}{\Phi_0} (2 \sinh \bar{\varphi}_i + \bar{\chi}_i^2 e^{\bar{\varphi}_i}) \mathcal{Y} - \frac{1}{2\Phi_0^4} \sum_{j \neq i} \left(\partial_{\bar{\varphi}_j} \partial_{\bar{\varphi}_i} \bar{V} \varphi_j + \partial_{\bar{\chi}_j} \partial_{\bar{\varphi}_i} \bar{V} \chi_j \right), \tag{33}$$

and

$$0 = e^{2\bar{\varphi}_i} \square \chi_i + \left(2g^2 e^{\bar{\varphi}_i} - \frac{1}{2\Phi_0^4} \partial_{\bar{\chi}_i}^2 \bar{V} \right) \chi_i + \frac{8g^2}{\Phi_0} \bar{\chi}_i e^{\bar{\varphi}_i} \mathcal{Y} - \frac{1}{2\Phi_0^4} \sum_{j \neq i} \left(\partial_{\bar{\chi}_j} \partial_{\bar{\chi}_i} \bar{V} \chi_j + \partial_{\bar{\varphi}_j} \partial_{\bar{\chi}_i} \bar{V} \varphi_j \right). \tag{34}$$

It is worth noting the different behaviour of the fluctuations for the gauged versus un-gauged theory. For $g = 0$, the fluctuations of (h_{ab}, \mathcal{Y}) are decoupled from the matter sector (φ_i, χ_i) . For $g \neq 0$, we have to decouple further the fluctuations. We will do so by splitting the solutions of (33) and (34) into a homogeneous and inhomogeneous part

$$\begin{aligned} \varphi_i &= \varphi_i^{\text{hom}} + \frac{a_{\varphi,i}}{\Phi_0} \mathcal{Y}, \\ \chi_i &= e^{-\bar{\varphi}_i} \chi_i^{\text{hom}} + e^{-\bar{\varphi}_i} \frac{a_{\chi,i}}{\Phi_0} \mathcal{Y}. \end{aligned} \tag{35}$$

The homogeneous terms in (35) satisfy at linear order

$$\begin{aligned} \square \varphi_i^{\text{hom}} &= \left(\frac{1}{\ell_2^2} + \frac{1}{\Phi_0^2} - g^2 (2 \cosh \bar{\varphi}_i + \bar{\chi}_i^2 e^{\bar{\varphi}_i}) \right) \varphi_i^{\text{hom}} \\ &+ \frac{1}{2\Phi_0^4} \sum_{j \neq i} \left(\partial_{\bar{\varphi}_j} \partial_{\bar{\varphi}_i} \bar{V} \varphi_j^{\text{hom}} + e^{-\bar{\varphi}_j} \partial_{\bar{\chi}_j} \partial_{\bar{\varphi}_i} \bar{V} \chi_j^{\text{hom}} \right), \end{aligned} \tag{36}$$

and

$$\begin{aligned} \square \chi_i^{\text{hom}} &= \left(\frac{1}{\ell_2^2} + \frac{1}{\Phi_0^2} - g^2 (2 \cosh \bar{\varphi}_i + \bar{\chi}_i^2 e^{\bar{\varphi}_i}) \right) \chi_i^{\text{hom}} \\ &+ \frac{1}{2\Phi_0^4} \sum_{j \neq i} \left(e^{-\bar{\varphi}_i - \bar{\varphi}_j} \partial_{\bar{\chi}_j} \partial_{\bar{\chi}_i} \bar{V} \chi_j^{\text{hom}} + e^{-\bar{\varphi}_i} \partial_{\bar{\varphi}_j} \partial_{\bar{\chi}_i} \bar{V} \varphi_j^{\text{hom}} \right). \end{aligned} \tag{37}$$

It will be convenient to introduce some further notation to encode the information of these linear equations. We will write (36) and (37) as

$$\square \vec{\psi}_h = \mathfrak{M}^2 \vec{\psi}_h, \tag{38}$$

where $\vec{\psi}_h \equiv (\varphi_i^{\text{hom}}, \chi_i^{\text{hom}})$, and \mathfrak{M}^2 is a 6×6 mass matrix that can be read off from the above equations. The coefficients $a_{\varphi,i}$ and $a_{\chi,i}$, which parametrise the inhomogeneous solution, are determined such that terms proportional to \mathcal{Y} in (33) and (34) are removed from the equations. The condition is

$$\left(\mathfrak{M}^2 - \frac{2}{\ell_2^2} \mathbb{1}_{6 \times 6} \right) \vec{a} = -4g^2 \vec{b}, \quad \vec{b} \equiv \begin{pmatrix} (2 \sinh \bar{\varphi}_i + \bar{\chi}_i^2 e^{\bar{\varphi}_i}) \\ 2\bar{\chi}_i \end{pmatrix}, \tag{39}$$

with $\vec{a} = (a_{\varphi,i}, a_{\chi,i})$. We will solve for \vec{a} explicitly for the cases in Section 5. Notice that for $g = 0$, the solution to (39) is $\vec{a} = 0$, reflecting that there is no inhomogeneous solution in that case.

Finally, from (20), we obtain the linearised equation for the metric fluctuation, h_{ab} , which reads

$$\begin{aligned}
 & -\bar{R}^{ab}h_{ab} + \bar{\nabla}^a\bar{\nabla}^bh_{ab} - \bar{\square}h^a_a - \left(\frac{8}{\ell_2^2} + \frac{4}{\Phi_0^2}\right)\mathcal{Y} \\
 & + 2g^2\Phi_0\sum_{i=1}^3\left(\left(2\sinh\bar{\varphi}_i + (\bar{\chi}_i)^2e^{\bar{\varphi}_i}\right)\varphi_i + 2e^{\bar{\varphi}_i}\bar{\chi}_i\chi_i\right) = 0.
 \end{aligned}
 \tag{40}$$

This equation reflects how the metric mixes with the JT field \mathcal{Y} , which is a standard feature of sphere reductions, and for $g \neq 0$, how the matter fields get intertwined as well. To disentangle this equation and identify the inhomogeneous piece H^{inh} , we start by writing

$$h_{ab} = \hat{h}_{ab}^{\text{ST}} + \frac{1}{2}\bar{g}_{ab}\hat{h} + \Phi_0\bar{g}_{ab}H^{\text{inh}}, \tag{41}$$

where \hat{h}_{ab}^{ST} is a symmetric traceless tensor, and \hat{h} , together with H^{inh} , describe the trace of the perturbation. It is simple to check that the inhomogeneous solution to (40) is

$$H^{\text{inh}} = \frac{1}{2}\bar{a} \cdot \bar{\psi}_h, \tag{42}$$

with \bar{a} given by (39), and

$$\bar{\square}\hat{h} = \frac{2}{\ell_2^2}\hat{h}. \tag{43}$$

However, notice that \hat{h} is not a new degree of freedom: this equation reflects the residual diffeomorphism that we can still do on the background metric [42]. Finally, from (40), the term \hat{h}_{ab}^{ST} obeys

$$\bar{\nabla}^a\bar{\nabla}^b\hat{h}_{ab}^{\text{ST}} - \left(\frac{8}{\ell_2^2} + \frac{4}{\Phi_0^2} - 2g^2\bar{b} \cdot \bar{a}\right)\mathcal{Y} = 0, \tag{44}$$

which couples the metric to \mathcal{Y} , and we will discuss the solutions when addressing the JT sector.

To summarise, the independent fluctuations around the AdS₂ backgrounds correspond to the JT field \mathcal{Y} and the matter sector containing $(\varphi_i^{\text{hom}}, \chi_i^{\text{hom}})$. For each matter degree of freedom, we will have a corresponding dual operator, and the six eigenvalues of the mass matrix in (38) will be related to the conformal dimensions of these operators in the standard way

$$\Delta_i = \frac{1}{2}\left(1 + \sqrt{1 + 4m_i^2\ell_2^2}\right), \tag{45}$$

with m_i^2 an eigenvalue of \mathfrak{M}^2 . This, plus $\Delta_{\mathcal{Y}} = 2$, corresponds to the spectrum of operators in our system.

JT sector. The JT sector is the portion of the fluctuations that is controlled by \mathcal{Y} , and the homogeneous solutions are trivial. More explicitly, in (30), we set

$$\begin{aligned}
 (\varphi_i, e^{\bar{\varphi}_i}\chi_i) &= \frac{\mathcal{Y}}{\Phi_0}\bar{a}, \\
 h_{ab} &= \hat{h}_{ab}^{\text{ST}},
 \end{aligned}
 \tag{46}$$

with \bar{a} the solution to (39), \hat{h}_{ab}^{ST} satisfies (44), and \mathcal{Y} is governed by (31). The dynamical aspects of \mathcal{Y} , defined by its distinctive equation of motion (31), are well described by JT gravity. Provided some assumptions on the operator content of the theory, this sector controls the deviations away from extremality, where it can be seen that a non-trivial profile of \mathcal{Y} accounts for the response of the black hole as the temperature is increased [1,43]. This has been well reported for spherically symmetric cases in four dimensions in [31,32] when the theory was only Einstein–Maxwell theory.

To complete the discussion of the JT sector, we will construct the solutions to (44). We will write the traceless part as

$$\hat{h}_{ab}^{ST} = \bar{\nabla}_a \bar{\nabla}_b U(x) - \frac{1}{2} g_{ab} \bar{\square} U(x), \tag{47}$$

with $U(x)$ a scalar function. Then (44) reduces to

$$\left(\bar{\square} - \frac{2}{\ell_2^2}\right)U(x) = \left(\frac{4}{\ell_2^2} + \frac{2}{\Phi_0^2} - g^2 \vec{b} \cdot \vec{a}\right)\mathcal{Y}. \tag{48}$$

Although we are describing the solution to \hat{h}_{ab}^{ST} in the context of the linearised equations, it is important to note that this backreaction of the geometry is a higher-order effect in powers of \mathcal{Y} . The reason is simply that (44) is obtained by varying the action with respect to \mathcal{Y} , and this requires terms that are schematically of the form $h\mathcal{Y} + \mathcal{Y}^2$. We will only focus on linear order effects in \mathcal{Y} , and hence (47) will not play a role in Section 3.3.

To close the analysis of this subsection, it is instructive to compare with prior results. In particular, refs. [42,44,45] contain a detailed study of the linearised spectrum of $\text{AdS}_2 \times S^2$ in the ungauged theory, which includes all possible harmonics on S^2 . Our analysis corresponds to the lowest $l = 0$ sector in their notation. One important difference is that [42,44] makes a choice of Lorentz, or de Donder, gauge in four dimensions; here, we have not fixed a gauge. This choice of gauge forces $\mathcal{Y} = 0$, and the JT dynamics appear as boundary modes. Otherwise, our analysis is in agreement with theirs.

3.3. Interactions in Near-AdS₂

Finally, we will focus on the interactions between \mathcal{Y} and the matter fields in our model. We will be treating \mathcal{Y} as a background field—with its non-trivial profile driving the system away from the ideal AdS_2 background by explicitly breaking conformal invariance—and we will quantify its imprint on the matter sector. In such a scenario, cubic interactions that involve one power of \mathcal{Y} capture the leading correction to the two-point functions, which we aim to evaluate.

In this subsection, we will only describe the general aspects of these interactions and how they enter in the two-point function of the matter sector; in the subsequent sections, we will evaluate these corrections explicitly for specific cases. The general strategy presented here follows the discussion in [5], which we summarise and apply to our situation.

To quantify these interactions, and their impact on two-point functions of the matter fields, we start by writing the bosonic supergravity fields as

$$\begin{aligned} \Phi &= \Phi_0 + \mathcal{Y}, \\ (\varphi_i, e^{\bar{\varphi}_i} \chi_i) &= (\bar{\varphi}_i, e^{\bar{\varphi}_i} \bar{\chi}_i) + \vec{a} \frac{\mathcal{Y}}{\Phi_0} + (\varphi_i, e^{\bar{\varphi}_i} \chi_i), \\ g_{ab} &= \Phi_0 \bar{g}_{ab} + \frac{\Phi_0}{2} \bar{g}_{ab} \vec{a} \cdot \vec{\psi}. \end{aligned} \tag{49}$$

Here $(\bar{g}_{ab}, \Phi_0, \bar{\varphi}_i, \bar{\chi}_i)$ specifies the AdS_2 background, which complies with the equations of motion in Section 3.1; the vector \vec{a} is defined in (39). We also have $\vec{\psi} \equiv (\varphi_i, \chi_i)$, which describes the matter degrees of freedom beyond the linearised level discussed in Section 3.2.

Starting from (18) and (19), we will build the effective action that captures the dynamics of $\vec{\psi}$, including interactions with the JT sector to leading order in \mathcal{Y} . This effective Euclidean action will be of the form

$$I_{\text{eff}} = \frac{\Phi_0^2}{4G_4} \int d^2x \sqrt{\bar{g}} (\mathcal{L}_{\text{free}} + \mathcal{L}_{\text{int}}), \tag{50}$$

where the free portion describes the quadratic action for $\vec{\psi}$

$$\mathcal{L}_{\text{free}} = \frac{1}{2} \partial_a \vec{\psi} \cdot \partial^a \vec{\psi} + \frac{1}{2} \vec{\psi}^T \mathfrak{M}^2 \vec{\psi}, \tag{51}$$

with the mass matrix as given by (38). In obtaining $\mathcal{L}_{\text{free}}$ it was important to introduce terms proportional to \vec{a} in (49), since otherwise, the matter degrees of freedom in $\vec{\psi}$ would not decouple from the gravitational degrees of freedom (\mathcal{Y}, h_{ab}) . As expected, the free terms capture the homogeneous solutions of the linearised spectrum in Section 3.2. The leading cubic interaction terms are⁶

$$\begin{aligned} \mathcal{L}_{\text{int}} = & \frac{1}{2} \partial_a \mathcal{Y} (\partial^a \vec{\psi} \cdot \vec{a}) \vec{\psi} \cdot \vec{a} + \mathcal{Y} \partial_a \vec{\psi} \cdot \partial^a \vec{\psi} \\ & + \frac{1}{2} \sum_{i=1}^3 (a_{\chi,i} \varphi_i \partial_a \mathcal{Y} \partial^a \chi_i + 2a_{\varphi,i} \mathcal{Y} \partial^a \chi_i \partial_a \chi_i) \\ & + \sum_{i,j=1}^6 \lambda_{\psi_i \psi_j \mathcal{Y}} \psi_i \psi_j \mathcal{Y}. \end{aligned} \tag{52}$$

The expression of $\lambda_{\psi_i \psi_j \mathcal{Y}}$, in terms of the background AdS₂ solution and \vec{a} , is rather lengthy for (18), and hence we are not writing it explicitly. However, it is straightforward to evaluate.

It will also be useful to bring (50) to a diagonal basis, where it is simple to read off the eigenvalues of \mathfrak{M}^2 . For this reason, we define $\vec{\mathfrak{z}}$, which contains the orthogonal eigenstates of \mathfrak{M}^2 . In this basis, (50) becomes

$$\begin{aligned} I_{\text{eff}} = & \int d^2x \sqrt{\bar{g}} \left(\frac{1}{2} \partial_a \vec{\mathfrak{z}} \cdot \partial^a \vec{\mathfrak{z}} + \frac{1}{2} \vec{\mathfrak{z}} M^2 \vec{\mathfrak{z}} \right. \\ & \left. + \sum_{i,j} \left(\lambda_{\mathfrak{z}_i \mathfrak{z}_j \mathcal{Y}} \mathfrak{z}_i \mathfrak{z}_j \mathcal{Y} + \lambda_{\mathfrak{z}_i (\partial \mathfrak{z}_j) (\partial \mathcal{Y})} \mathfrak{z}_i \partial_a \mathfrak{z}_j \partial^a \mathcal{Y} + \lambda_{\mathcal{Y} (\partial \mathfrak{z}_i) (\partial \mathfrak{z}_j)} \mathcal{Y} \partial_a \mathfrak{z}_i \partial^a \mathfrak{z}_j \right) \right). \end{aligned} \tag{53}$$

Here $M^2 = \text{diag}(m_1^2, \dots, m_6^2)$ contains, in its diagonal, the eigenvalues of \mathfrak{M}^2 , and the cubic couplings appearing above will follow. Furthermore, note that $\vec{\mathfrak{z}}$ has been appropriately normalised to remove the overall factor of $\frac{\Phi_0^2}{4G_4}$ in (50).

Next, let us focus on the evaluation of the two-point function of one of the eigenstates in (53), which for the sake of simplicity (and abusing notation) we will call $\mathfrak{z}(x)$, and whose mass eigenvalue within M^2 is $m_{\mathfrak{z}}^2$. To start, in the vacuum (pure AdS in the bulk), we can use coordinates such that

$$ds_{\text{AdS}_2}^2 = \frac{\ell_2^2}{z^2} (dt^2 + dz^2). \tag{54}$$

In these coordinates, the near-boundary expansion of \mathfrak{z} is

$$\mathfrak{z}(t, z) = z^{1-\Delta} \vec{\mathfrak{z}}(t) + \dots, \quad \text{as } z \rightarrow 0, \tag{55}$$

and $\vec{\mathfrak{z}}(t)$ is interpreted as the source of its dual operator $\mathcal{O}_{\mathfrak{z}}(t)$ with dimension

$$\Delta \equiv \Delta_{\mathfrak{z}} = \frac{1}{2} \left(1 + \sqrt{1 + 4m_{\mathfrak{z}}^2 \ell_2^2} \right). \tag{56}$$

Next, we can perform a diffeomorphism in the bulk to go to a thermal state, with inverse temperature β . Near the boundary, the appropriate thermal transformation is

$$t(u) = \tan\left(\frac{\pi}{\beta} u\right), \quad u \sim u + \beta, \tag{57}$$

with u being the boundary time. As we do this transformation, we also want to keep track of the UV cut-off and make sure the proper length of the boundary is fixed, i.e.,

$$g|_{\text{bdy}} = \frac{\ell_2^2}{\epsilon^2}. \tag{58}$$

The above condition implies that

$$z(u) = \epsilon \sqrt{(t')^2 + (z')^2} = \epsilon t(u)' + \mathcal{O}(\epsilon^3), \tag{59}$$

fixing the asymptotic part of the radial part of the diffeomorphism. Then, under this transformation, the asymptotic form of the field \mathfrak{z} becomes

$$\mathfrak{z}(t, z) = \epsilon^{1-\Delta} [t'(u)]^{1-\Delta} \tilde{\mathfrak{z}}(t(u)) + \dots, \quad \text{as } \epsilon \rightarrow 0, \tag{60}$$

and now $[t'(u)]^{1-\Delta} \tilde{\mathfrak{z}}(t(u)) \equiv \bar{\mathfrak{z}}(u)$ is interpreted as a source.

Turning next to the behavior of \mathcal{Y} , this term will be treated as a background field whose source is non-trivial. More explicitly, we will take the on-shell value⁷

$$\Phi_0^{-1} \mathcal{Y}(t, z) = z^{-1} \tilde{\mathcal{Y}}(t) + \dots \tag{61}$$

and set the source on the thermal state fixed, i.e., $\tilde{\mathcal{Y}}(u) = a$ with a a constant. This defines a near-AdS₂ background. Then, evaluating the two-point functions of the operator dual to \mathfrak{z} in the presence of a background value for \mathcal{Y} can be done by treating \mathcal{Y} as an operator with $\Delta = -1$, and integrating over its boundary time [2]. More explicitly, the thermal two-point function we are after is, to leading order in \mathcal{Y} ,

$$\langle \mathcal{O}_{\mathfrak{z}}(u_1) \mathcal{O}_{\mathfrak{z}}(u_2) \rangle_{\beta} = \langle \mathcal{O}_{\mathfrak{z}}(u_1) \mathcal{O}_{\mathfrak{z}}(u_2) \rangle_{\beta}^{\text{free}} + \langle \mathcal{O}_{\mathfrak{z}}(u_1) \mathcal{O}_{\mathfrak{z}}(u_2) \rangle_{\beta}^{\text{int}}, \tag{62}$$

where the correction due to \mathcal{Y} is

$$\langle \mathcal{O}_{\mathfrak{z}}(u_1) \mathcal{O}_{\mathfrak{z}}(u_2) \rangle_{\beta}^{\text{int}} = a \int_0^{\beta} du_3 \langle \mathcal{O}_{\mathfrak{z}}(u_1) \mathcal{O}_{\mathfrak{z}}(u_2) \mathcal{O}_{-1}(u_3) \rangle_{\beta}. \tag{63}$$

We can now easily evaluate the appropriate two-point function. As standard in AdS/CFT, the boundary effective action on the vacuum (54) is

$$I_{\text{eff}} = I_{\text{free}} + I_{\text{interactions}}. \tag{64}$$

The free part yields

$$I_{\text{free}} = -\frac{D}{2} \int dt_1 dt_2 \frac{\tilde{\mathfrak{z}}(t_1) \tilde{\mathfrak{z}}(t_2)}{|t_1 - t_2|^{2\Delta_3}}, \quad D = \frac{(2\Delta - 1)\Gamma[\Delta]}{\sqrt{\pi}\Gamma[\Delta - \frac{1}{2}]}. \tag{65}$$

The thermal two-point function is

$$\langle \mathcal{O}_{\mathfrak{z}}(u_1) \mathcal{O}_{\mathfrak{z}}(u_2) \rangle_{\beta}^{\text{free}} = D \left[\frac{t'(u_1)t'(u_2)}{|t(u_1) - t(u_2)|^2} \right]^{\Delta} = D \left[\frac{\pi}{\beta \sin\left(\frac{\pi u_{12}}{\beta}\right)} \right]^{2\Delta}, \tag{66}$$

where $u_{12} \equiv u_1 - u_2$. For the cubic interactions we will have

$$\begin{aligned} I_{\text{int}} &= \frac{\tilde{D}}{2} \int \frac{dt_1 dt_2 dt_3 \tilde{\mathfrak{z}}(t_1) \tilde{\mathfrak{z}}(t_2) \tilde{\mathcal{Y}}(t_3)}{|t_{12}|^{2\Delta+1} |t_{23}|^{-1} |t_{31}|^{-1}} \\ &= \frac{\tilde{D}}{2} \int du_1 du_2 du_3 \frac{t'(u_1)^{\Delta} t'(u_2)^{\Delta} t'(u_3)^{-1} \tilde{\mathfrak{z}}(u_1) \tilde{\mathfrak{z}}(u_2) \tilde{\mathcal{Y}}(u_3)}{|t(u_1) - t(u_2)|^{2\Delta+1} |t(u_1) - t(u_3)|^{-1} |t(u_2) - t(u_3)|^{-1}}, \end{aligned} \tag{67}$$

where

$$\tilde{D} \equiv \lambda_{\mathcal{Y}\mathfrak{z}\mathfrak{z}} K_{\mathcal{Y}\mathfrak{z}\mathfrak{z}} + \lambda_{\mathfrak{z}(\partial\mathfrak{z})(\partial\mathcal{Y})} K_{\mathfrak{z}(\partial\mathfrak{z})(\partial\mathcal{Y})} + \lambda_{\mathcal{Y}(\partial\mathfrak{z})(\partial\mathfrak{z})} K_{\mathcal{Y}(\partial\mathfrak{z})(\partial\mathfrak{z})}, \tag{68}$$

and the coefficients appearing here are [46]

$$\begin{aligned}
 K_{\mathcal{Y}33} &= -\frac{\Gamma[-\frac{1}{2}]^2\Gamma[\Delta + \frac{1}{2}]\Gamma[\Delta - 1]}{2\pi\Gamma[\Delta - \frac{1}{2}]^2\Gamma[-\frac{3}{2}]} = -\frac{3(\Delta - \frac{1}{2})\Gamma[\Delta - 1]}{2\sqrt{\pi}\Gamma[\Delta - \frac{1}{2}]}, \\
 K_{\mathfrak{z}(\partial\mathfrak{z})(\partial\mathcal{Y})} &= \left[-\Delta + \frac{1}{2}(2 - 2\Delta)(-1)\right] K_{\mathcal{Y}33} \ell_2^2 = -\frac{K_{\mathcal{Y}33}}{\ell_2^2}, \\
 \tilde{K}_{\mathcal{Y}(\partial\mathfrak{z})(\partial\mathfrak{z})} &= \left[\Delta^2 + \frac{1}{2}(2 - 2\Delta)(2\Delta + 1)\right] \frac{K_{\mathcal{Y}33}}{\ell_2^2} = -(\Delta^2 - \Delta - 1) \frac{K_{\mathcal{Y}33}}{\ell_2^2}.
 \end{aligned}
 \tag{69}$$

Then, the three-point function we need is

$$\langle \mathcal{O}_{\mathfrak{z}}(u_1)\mathcal{O}_{\mathfrak{z}}(u_2)\mathcal{O}_{-1}(u_3) \rangle_{\beta} = \tilde{D} \frac{\beta}{\pi} \left[\frac{\pi}{\beta \sin\left(\frac{\pi u_{12}}{\beta}\right)} \right]^{2\Delta} \frac{|\sin\left(\frac{\pi u_{13}}{\beta}\right)| |\sin\left(\frac{\pi u_{23}}{\beta}\right)|}{|\sin\left(\frac{\pi u_{12}}{\beta}\right)|},
 \tag{70}$$

which contributes to the correlator as

$$\begin{aligned}
 \langle \mathcal{O}_{\mathfrak{z}}(u_1)\mathcal{O}_{\mathfrak{z}}(u_2) \rangle_{\beta}^{\text{int}} &= a \int_0^{\beta} du_3 \langle \mathcal{O}_{\mathfrak{z}}(u_1)\mathcal{O}_{\mathfrak{z}}(u_2)\mathcal{O}_{-1}(u_3) \rangle_{\beta} \\
 &= \tilde{D} \frac{a\beta^2}{2\pi^2} \left[\frac{\pi}{\beta \sin\left(\frac{\pi u_{12}}{\beta}\right)} \right]^{2\Delta} \left(2 + \pi \frac{1 - 2u_{12}/\beta}{\tan\left(\frac{\pi u_{12}}{\beta}\right)} \right).
 \end{aligned}
 \tag{71}$$

See [5] for details about evaluating this integral. Adding the free and interaction pieces of the correlator, we find

$$\langle \mathcal{O}_{\mathfrak{z}}(u_1)\mathcal{O}_{\mathfrak{z}}(u_2) \rangle_{\beta} = \left[\frac{\pi}{\beta \sin\left(\frac{\pi u_{12}}{\beta}\right)} \right]^{2\Delta} \left[D + \tilde{D} \frac{a\beta^2}{2\pi^2} \left(2 + \pi \frac{1 - 2u_{12}/\beta}{\tan\left(\frac{\pi u_{12}}{\beta}\right)} \right) \right].
 \tag{72}$$

The constants D and \tilde{D} are given in (65) and (68), respectively.

As we investigate examples in the subsequent sections, one of our main aims will be to report on the value of \tilde{D} compared to D . For this purpose, it is convenient to define their ratio as

$$\hat{D} \equiv \frac{\tilde{D}}{D} = \frac{\lambda_{\text{eff}} K_{\mathcal{Y}33}}{D} = -\frac{3}{4(\Delta - 1)} \lambda_{\text{eff}},
 \tag{73}$$

where $\lambda_{\text{eff}} = \lambda_{\text{eff}}(\Delta)$ is the effective cubic coupling constant, which depends on the conformal dimension of \mathfrak{z} via (69). We will see that the value of \hat{D} behaves differently depending on the background and surrounding: BPS versus non-BPS backgrounds, gauged versus ungauged theories. Understanding what the possible behaviours are is valuable information to understand how specific properties of the dual system accommodate for the properties of the gravitational background.

4. Ungauged Supergravity

It is instructive to specialise to the case $g = 0$ and inspect more closely the responses and fluctuations of extremal black holes. The main goal here is two-fold: first, to recover the aspects of the nAttractor mechanism, and second, to contrast the response of near-AdS₂ of BPS versus non-BPS black holes. We will start this section by describing the BPS and non-BPS branches; subsequently, we will describe the IR fixed point and the linear analysis, classifying the solutions according to them being BPS or non-BPS. Finally, we study the interactions between the scalars and axions and the dilaton field \mathcal{Y} , highlighting the differences between both branches.

There are multiple references to characterise the $\mathcal{N} = 2$ ungauged supergravity theories at hand and several different conventions used in those references, which we will not summarise here. By setting $g = 0$ for the theory presented in Section 2.1, one obtains STU supergravity described according to the conventions in [19], and those are the conventions used here.

4.1. BPS Versus Non-BPS Branch

For ungauged black holes, it is interesting to distinguish, among extremal black holes, which ones preserve supersymmetry (BPS branch) and which do not (non-BPS branch). For regular and static black holes, this distinction is elegantly dictated by the Cayley hyperdeterminant. This quantity is the quartic invariant of STU supergravity, and it is defined as [47,48]

$$\hat{\Delta} \equiv \frac{1}{16} \left(4Q_1 Q_2 Q_3 Q_4 + 4P^1 P^2 P^3 P^4 + 2 \sum_{J < K} Q_J Q_K P^J P^K - \sum_I (Q_I P^I)^2 \right). \tag{74}$$

One of the prominent roles played by this hyperdeterminant is that it controls the area of the extremal black hole and hence the Bekenstein–Hawking entropy of it

$$S_{\text{BH,ext}} = \frac{\pi}{G_4} \Phi_0^2 = \frac{2\pi}{G_4} \sqrt{|\hat{\Delta}|}. \tag{75}$$

Another utility of this invariant is that we can identify two branches of solutions: an extremal black hole in STU supergravity can then be labelled as

$$\begin{aligned} \text{non - BPS} : \quad & \hat{\Delta} < 0, \\ \text{BPS} : \quad & \hat{\Delta} > 0. \end{aligned} \tag{76}$$

The case $\hat{\Delta} = 0$ is singular for black holes in a two-derivative supergravity theory since the horizon area vanishes; these configurations are usually referred to as a small black hole.

4.2. AdS₂ Background: IR Fixed Point

When $g = 0$, the system becomes much more manageable: it is simpler to quantify the background and the fluctuations around it. For the AdS₂ background, the main simplification comes from the second equation in (26), which gives

$$\ell_2^2 = \Phi_0^2, \tag{77}$$

implying that the AdS₂ and S² radii are equal to each other. Then, the conditions on the constant scalars supporting the AdS₂ gives

$$\partial_{\bar{\chi}_i} \bar{V} = \partial_{\bar{\varphi}_i} \bar{V} = 0, \tag{78}$$

which are the renowned conditions from the attractor mechanism of extremal black holes; see, for example, refs. [11,13] for a general analysis. Explicitly, they are given by (A18) and (A19) with $g = 0$ for the ungauged theory considered here.

For what follows, it will be useful to rewrite the expression for the Cayley hyperdeterminant in terms of the charges dressed by the moduli: $(\mathcal{P}^I, \mathcal{Q}_I)$ defined in (A15)–(A17). The expression (74) becomes

$$\hat{\Delta} = \frac{e^{-2(\bar{\varphi}_1 + \bar{\varphi}_2 + \bar{\varphi}_3)}}{16} \left(4\mathcal{Q}_1 \mathcal{Q}_2 \mathcal{Q}_3 \mathcal{Q}_4 + 4\mathcal{P}^1 \mathcal{P}^2 \mathcal{P}^3 \mathcal{P}^4 + 2 \sum_{J < K} \mathcal{Q}_J \mathcal{Q}_K \mathcal{P}^J \mathcal{P}^K - \sum_I (\mathcal{Q}_I \mathcal{P}^I)^2 \right). \tag{79}$$

It is also simpler to discuss the solutions to the attractor equations (78) in terms of $(\mathcal{P}^I, \mathcal{Q}_I)$. In this notation, the BPS branch ($\hat{\Delta} > 0$) of solutions is very simple and dictated by the linear conditions as follows. First, a solution to (78) can be obtained by demanding⁸

$$|\mathcal{P}^1| = |\mathcal{P}^2| = |\mathcal{P}^3| = |\mathcal{P}^4|, \quad \text{and} \quad |\mathcal{Q}_1| = |\mathcal{Q}_2| = |\mathcal{Q}_3| = |\mathcal{Q}_4|. \tag{80}$$

Second, to make this a BPS solution, one has to select an even number of minus signs, and the signs of the \mathcal{P}^I and Q_I are matched. For example, one possible BPS solution is of the form

$$\mathcal{P}^1 = \mathcal{P}^2 = -\mathcal{P}^3 = -\mathcal{P}^4, \quad Q_1 = Q_2 = -Q_3 = -Q_4. \tag{81}$$

Without a loss of generality, we will use this choice of signs as a representative of the BPS branch in what follows.

In the non-BPS branch ($\hat{\Delta} < 0$), solutions of the form (80) also exist, but with an odd number of relative minus signs for both Q_I and \mathcal{P}^I ; contrary to the BPS branch, the signs do not have to be matched. One example of this class of solutions is

$$\mathcal{P}^1 = -\mathcal{P}^2 = -\mathcal{P}^3 = -\mathcal{P}^4, \quad Q_1 = Q_2 = -Q_3 = Q_4. \tag{82}$$

However, there exist non-BPS solutions to (78) that do not comply (or only partially comply) with the conditions (80). In Appendix D, we will comment on this other class of non-BPS attractor solutions and how both BPS and non-BPS configurations can be obtained as the extremal limit of the black hole solutions discussed in [19].

Lastly, the AdS₂ radius (26), or (A20), in terms of (\mathcal{P}^I, Q_I) is given by

$$\ell_2^2 = \frac{1}{4} e^{-\bar{\varphi}_1 - \bar{\varphi}_2 - \bar{\varphi}_3} \left(Q_1^2 + Q_2^2 + Q_3^2 + Q_4^2 + (\mathcal{P}^4)^2 + (\mathcal{P}^3)^2 + (\mathcal{P}^2)^2 + (\mathcal{P}^1)^2 \right). \tag{83}$$

Furthermore, also note that $\ell_2^2 = \sqrt{|\hat{\Delta}|}$. For both BPS and non-BPS solutions of the type (80), we can simplify this expression further, which reads

$$\ell_2^2 = e^{-\bar{\varphi}_1 - \bar{\varphi}_2 - \bar{\varphi}_3} \left((\mathcal{P}^1)^2 + (Q_1)^2 \right). \tag{84}$$

4.3. Linear Analysis

In this section, we revisit the linear analysis performed in Section 3.2. As noted there, several simplifications occur on the spectrum of fluctuations when $g = 0$; the most prominent one being that we do not have inhomogeneous terms that mix the JT field with the matter content. In the following, we will gather those expressions and solve them for the BPS and non-BPS backgrounds discussed in Section 4.2.

We will cast the perturbations as

$$\begin{aligned} \Phi &= \Phi_0 + \mathcal{Y}, \\ \varphi_i &= \bar{\varphi}_i + \boldsymbol{\varphi}_i^{\text{hom}}, \\ \chi_i &= \bar{\chi}_i + e^{-\bar{\varphi}_i} \boldsymbol{\chi}_i^{\text{hom}}, \\ g_{ab} &= \Phi_0 \bar{g}_{ab} + \hat{h}_{ab}, \end{aligned} \tag{85}$$

reflecting that we do not have inhomogeneous terms present in (35) and (41). In the following we will just replace $\boldsymbol{\varphi}_i^{\text{hom}} \rightarrow \boldsymbol{\varphi}_i$ and $\boldsymbol{\chi}_i^{\text{hom}} \rightarrow \boldsymbol{\chi}_i$, since the label is redundant here. As usual, \mathcal{Y} is the JT field, obeying (31). For the metric fluctuations in (44), we have

$$\bar{\nabla}^a \bar{\nabla}^b \hat{h}_{ab} - \bar{\square} \hat{h}_a^a + \frac{2}{\ell_2^2} \hat{h}_a^a - \frac{12}{\ell_2^2} \mathcal{Y} = 0, \tag{86}$$

and the linear equations for the scalar fields (33) and (34) simplify to

$$\begin{aligned} 0 &= \left(\bar{\square} - \frac{2}{\ell_2^2} \right) \boldsymbol{\varphi}_i - \frac{1}{2\ell_2^4} \sum_{j \neq i} \left(\partial_{\bar{\varphi}_j} \partial_{\bar{\varphi}_i} \bar{V} \boldsymbol{\varphi}_j + \partial_{\bar{\chi}_j} \partial_{\bar{\varphi}_i} \bar{V} \boldsymbol{\chi}_j \right), \\ 0 &= \left(\bar{\square} - \frac{2}{\ell_2^2} \right) \boldsymbol{\chi}_i - \frac{e^{-2\bar{\varphi}_i}}{2\ell_2^4} \sum_{j \neq i} \left(\partial_{\bar{\chi}_j} \partial_{\bar{\chi}_i} \bar{V} \boldsymbol{\chi}_j + \partial_{\bar{\varphi}_j} \partial_{\bar{\chi}_i} \bar{V} \boldsymbol{\varphi}_j \right). \end{aligned} \tag{87}$$

Our main aim is to determine the mass eigenvalues and eigenvectors of (87); with this, we will quantify the dual operators that should be part of the holographic description of the near-extremal black hole. Focusing first on the attractor solutions characterised by (80), then we have

$$\bar{\square}\vec{\psi} - \mathfrak{M}^2\vec{\psi} = 0, \tag{88}$$

where $\vec{\psi} = (\varphi_i, \chi_i)$, and the mass matrix \mathfrak{M}^2 is given by

$$\mathfrak{M}^2 = \frac{2}{\ell_2^2} \begin{pmatrix} 1 & 0 & 0 & 0 & m_{15} & m_{16} \\ 0 & 1 & 0 & m_{24} & 0 & m_{26} \\ 0 & 0 & 1 & m_{34} & m_{35} & 0 \\ 0 & m_{24} & m_{34} & 1 & m_{45} & m_{46} \\ m_{15} & 0 & m_{35} & m_{45} & 1 & m_{56} \\ m_{16} & m_{26} & 0 & m_{46} & m_{56} & 1 \end{pmatrix}, \tag{89}$$

with

$$\begin{aligned} m_{15} &= \alpha(\mathcal{P}^4 Q_2 - \mathcal{P}^1 Q_3), & m_{35} &= \alpha(\mathcal{P}^4 Q_2 - \mathcal{P}^3 Q_1), \\ m_{16} &= \alpha(\mathcal{P}^4 Q_3 - \mathcal{P}^1 Q_2), & m_{45} &= \frac{\alpha}{2}(\mathcal{P}^4 \mathcal{P}^3 - Q_1 Q_2 - \mathcal{P}^1 \mathcal{P}^2 + Q_3 Q_4), \\ m_{24} &= \alpha(\mathcal{P}^4 Q_1 - \mathcal{P}^2 Q_3), & m_{46} &= \frac{\alpha}{2}(\mathcal{P}^4 \mathcal{P}^2 - Q_1 Q_3 - \mathcal{P}^1 \mathcal{P}^3 + Q_2 Q_4), \\ m_{26} &= \alpha(\mathcal{P}^4 Q_3 - \mathcal{P}^2 Q_1), & m_{56} &= \frac{\alpha}{2}(\mathcal{P}^4 \mathcal{P}^1 - Q_2 Q_3 - \mathcal{P}^2 \mathcal{P}^3 + Q_1 Q_4), \\ m_{34} &= \alpha(\mathcal{P}^4 Q_1 - \mathcal{P}^3 Q_2), & & \end{aligned} \tag{90}$$

where

$$\alpha = -\frac{1}{(\mathcal{P}^1)^2 + (Q_1)^2}. \tag{91}$$

We can now diagonalise the mass matrix such that

$$\bar{\square}\vec{\mathfrak{z}} - M^2\vec{\mathfrak{z}} = 0, \tag{92}$$

where M^2 is the matrix with the mass eigenvalues of \mathfrak{M}^2 , and $\vec{\mathfrak{z}}$ are its eigenvectors. From the definition of the BPS branch, it is clear that all non-diagonal matrix elements (90) vanish, and the mass matrix is automatically diagonal. In the non-BPS branch, \mathfrak{M}^2 also simplifies further: depending on the precise distribution of minus signs, m_{15} to m_{35} evaluate to

$$\pm 2\alpha\mathcal{P}^1 Q_1 \quad \text{or} \quad 0, \tag{93}$$

and m_{45}, m_{46} , and m_{56} evaluate to

$$\pm \alpha((\mathcal{P}^1)^2 - (Q_1)^2) \quad \text{or} \quad 0. \tag{94}$$

Hence, depending on the assignment of minus signs in (80), the eigenvalues of \mathfrak{M}^2 are

$$\text{BPS :} \quad M^2 = \text{diag}\left(\frac{2}{\ell_2^2}, \dots, \frac{2}{\ell_2^2}\right), \tag{95}$$

$$\text{non - BPS :} \quad M^2 = \text{diag}\left(0, 0, \frac{2}{\ell_2^2}, \frac{2}{\ell_2^2}, \frac{2}{\ell_2^2}, \frac{6}{\ell_2^2}\right). \tag{96}$$

Although the mass matrix is more complicated for the non-BPS solutions that do not obey (80) but instead have, for example, a solution to (78) with all \mathcal{P}^I and Q_I different, we confirmed numerically that the eigenvalues are still given by (96), and also for other non-BPS solutions. See Appendix D for details. For this reason, we expect that (96) captures the spectrum of fluctuations for any non-BPS configuration in STU models.

In the BPS branch, the eigenvectors are simply the scalar fields themselves. In the non-BPS branch, the eigenvectors are linear combinations of the fields (φ_i, χ_i) . As an illustrative example, for the case (82), the six eigenstates $\vec{\mathfrak{z}} = (\mathfrak{z}_1, \dots, \mathfrak{z}_6)$ are

$$\begin{aligned}
 m^2 \ell_2^2 = 0 \ (\Delta = 1) : \quad & \mathfrak{z}_1 = \chi_1 + \chi_3, \\
 & \mathfrak{z}_2 = -\frac{2\mathcal{P}^1 \mathcal{Q}_1}{(\mathcal{P}^1)^2 + (\mathcal{Q}_1)^2} \varphi_2 + \chi_1 + \frac{(\mathcal{P}^1)^2 - (\mathcal{Q}_1)^2}{(\mathcal{P}^1)^2 + (\mathcal{Q}_1)^2} \chi_2, \\
 m^2 \ell_2^2 = 2 \ (\Delta = 2) : \quad & \mathfrak{z}_3 = \varphi_1, \\
 & \mathfrak{z}_4 = \varphi_3, \\
 & \mathfrak{z}_5 = \left((\mathcal{P}^1)^2 - (\mathcal{Q}_1)^2 \right) \varphi_2 + 2\mathcal{P}^1 \mathcal{Q}_1 \chi_2, \\
 m^2 \ell_2^2 = 6 \ (\Delta = 3) : \quad & \mathfrak{z}_6 = -\frac{2\mathcal{P}^1 \mathcal{Q}_1}{(\mathcal{P}^1)^2 + (\mathcal{Q}_1)^2} \varphi_2 - \chi_1 + \frac{(\mathcal{P}^1)^2 - (\mathcal{Q}_1)^2}{(\mathcal{P}^1)^2 + (\mathcal{Q}_1)^2} \chi_2 + \chi_3.
 \end{aligned} \tag{97}$$

To avoid clutter, here we wrote eigenstates \mathfrak{z}_i that are not orthogonal, and we have not included the appropriate normalisation to comply with (53). When discussing interactions in Section 4.5, we will be referring to a basis that is orthogonal and normalised correctly. We also note that this spectrum is in perfect agreement with the non-BPS branch spectrum analysed in [45].

It is interesting to connect the spectrum of the non-BPS branch to the five-dimensional analysis in [41]. When reducing the ungauged five-dimensional theory along a circle, the Myers–Perry black hole can be viewed as an electrically charged solution; its D-brane construction corresponds to the D0+D6 system, as first noted in [49]. In the context of the spectrum, we note that the state with $\Delta = 3$ here is precisely the squashing mode χ in [41].

4.4. nAttractor Revisited

It is interesting to place our linear analysis in the context of the nAttractor mechanism proposed in [16]. The observation of the nAttractor is that generic scalar moduli, in our case (φ_i, χ_i) , should respond in the near-AdS₂ region as

$$\begin{aligned}
 \varphi_i &= \bar{\varphi}_i + \frac{\varphi_i^{(1)}}{z} + \dots, \\
 \chi_i &= \bar{\chi}_i + \frac{\chi_i^{(1)}}{z} + \dots,
 \end{aligned} \quad \text{as } z \rightarrow 0, \tag{98}$$

where $(\bar{\varphi}_i, \bar{\chi}_i)$ are the attractor values of the scalars, and $(\varphi_i^{(1)}, \chi_i^{(1)})$ are constants. The power in the AdS₂ radial direction z was used as evidence to argue that each of the scalar moduli is dual to an irrelevant operator of conformal dimension $\Delta = 2$.

For the fluctuations around BPS backgrounds, this is indeed true: we showed explicitly that the dilaton and axion perturbations, φ_i and χ_i , are eigenstates with masses $m^2 = \frac{2}{\ell_2^2}$ and corresponding conformal dimensions $\Delta = 2$.⁹ Therefore, they have a response as in (98) as one moves away from the AdS₂ background, in perfect agreement with the nAttractor. Despite sharing the same conformal dimension as \mathcal{Y} , it should be noted that these modes stand on a different footing: only \mathcal{Y} obeys the constrained JT equation (31), which ties its response to thermal AdS₂ and the Schwarzian action.

For the non-BPS solutions, the relation to the nAttractor is not as simple. In this case we found that the spectrum of fluctuations contains mass eigenstates with $m^2 = 0$, $m^2 = \frac{2}{\ell_2^2}$, and $m^2 = \frac{6}{\ell_2^2}$, corresponding to a conformal dimension $\Delta = 1$, $\Delta = 2$ or $\Delta = 3$, respectively. This implies that the eigenstates that are unique to the non-BPS branch behave as

$$\begin{aligned}
 m^2 \ell_2^2 = 0 \ (\Delta = 1) : \quad & \mathfrak{z}_i = \mathfrak{z}_i^{(1)} + O(z^{-2}) \\
 m^2 \ell_2^2 = 6 \ (\Delta = 3) : \quad & \mathfrak{z}_i = \frac{\mathfrak{z}_i^{(1)}}{z^2} + \dots.
 \end{aligned} \tag{99}$$

Hence the marginal operator ($\Delta = 0$) could modify the attractor value, and the irrelevant operator with $\Delta = 6$ has a different imprint relative to \mathcal{Y} .

Two comments are in order regarding the non-BPS branch:

- The behaviour (98) persists for non-BPS black holes, as can be seen explicitly from the solutions in [19]. However, this is not enough to establish that the eigenstates are dual to operators with $\Delta = 2$. The reason is that $\varphi_i^{(1)}$ and $\chi_i^{(1)}$ are not independent parameters and cancellations occur. In Appendix D, we set up the extremal and near-horizon limit for the solutions in [19]: we show how combinations of $\varphi_i^{(1)}$ and $\chi_i^{(1)}$ cancel for non-BPS black holes and lead to the behaviour in (99).
- Having a marginal deformation means that there are flat directions in the attractor mechanism for non-BPS black holes. Concretely, the linear combinations of the attractor values of the scalars corresponding to the eigenstates with $m^2 = 0$ will not be fixed, but can instead take on different (constant) values. The eigenstates with $m^2 \neq 0$ will dictate which linear combinations cannot change in value. In the context of non-supersymmetric attractors, the occurrence of flat directions was reported initially in [15], and it could lead to potential instabilities of the system [53].

Finally, it is appropriate to add a comment about the gauged solutions and their behaviour in the context of the nAttractor. In that case, we can already see in a simple manner that (98) applies to the moduli, but for slightly different reasons. In the analysis of linear fluctuations in Section 3.2, we have an inhomogeneous solution for the scalar moduli in (35), which implies that the moduli behave in the near-AdS₂ region as

$$(\varphi_i, e^{\tilde{\varphi}_i} \chi_i) = (\bar{\varphi}_i, e^{\tilde{\varphi}_i} \bar{\chi}_i) + \vec{a} \frac{\mathcal{Y}}{\Phi_0} + (\varphi_i, e^{\tilde{\varphi}_i} \chi_i), \tag{100}$$

with the second term complying with (98). This is also evident if one inspects non-extremal black holes in gauged supergravity.¹⁰ However, in this case, it is also clear that the moduli do not have $\Delta = 2$: there is just a mixing of the JT field with the matter sector that needs to be diagonalised. The operator interpretation of the moduli comes from (φ_i, χ_i) , which contain the independent degrees of freedom.

4.5. Interactions

The classification of the interactions is relatively simple in the ungauged case, since the JT sector does not mix with the matter fields at the linear level. The effective Euclidean action for the matter fields around the near-AdS₂ background is of the form

$$I_{\text{eff}} = \int d^2x \sqrt{-\bar{g}^{(2)}} (\mathcal{L}_{\text{kin}} + \mathcal{L}_{\text{int}-\mathcal{Y}}), \tag{101}$$

The quadratic terms for the scalar fields, which contain the kinetic and mass terms, are

$$\mathcal{L}_{\text{kin}} = \frac{1}{2} \partial_a \vec{\mathfrak{z}} \cdot \partial^a \vec{\mathfrak{z}} + \frac{1}{2} \vec{\mathfrak{z}}^T M^2 \vec{\mathfrak{z}}. \tag{102}$$

Here $\vec{\mathfrak{z}}$ contains the degrees of freedom for the supergravity fields (φ_i, χ_i) and are orthogonal at leading order in the near-AdS₂ region; M^2 is the matrix with the mass eigenvalues as defined in (92). We are interested in finding the corrections to the two-point functions of the fields $\vec{\mathfrak{z}}$ due to the interactions with \mathcal{Y} discussed in (53). The terms in the effective action that involve cubic interactions with one power of \mathcal{Y} are very simple for the ungauged theory, and read

$$\mathcal{L}_{\text{int}} = \frac{1}{\Phi_0} \mathcal{Y} \partial_a \vec{\mathfrak{z}} \cdot \partial^a \vec{\mathfrak{z}} - \frac{3}{2\Phi_0} \mathcal{Y} \vec{\mathfrak{z}}^T M^2 \vec{\mathfrak{z}}. \tag{103}$$

As we discussed in Section 3.3, we want to report on how these interactions affect the two-point functions of $\vec{\mathfrak{z}}$. The final answer is of the form

$$\langle \mathcal{O}_{\mathfrak{z}_i}(u_1)\mathcal{O}_{\mathfrak{z}_i}(u_2) \rangle_\beta = \left[\frac{\pi}{\beta \sin\left(\frac{\pi u_{12}}{\beta}\right)} \right]^{2\Delta} \left[D + \frac{\tilde{D}a\beta^2}{2\pi^2} \left(2 + \pi \frac{1 - 2u_{12}/\beta}{\tan\left(\frac{\pi u_{12}}{\beta}\right)} \right) \right]. \tag{104}$$

Following from (68), the parameter \tilde{D} for this case is

$$\tilde{D} = \lambda_{\mathcal{Y}\mathfrak{z}_i\mathfrak{z}_i}K_{\mathcal{Y}\mathfrak{z}_i\mathfrak{z}_i} + \lambda_{\mathcal{Y}(\partial\mathfrak{z}_i)(\partial\mathfrak{z}_i)}K_{\mathcal{Y}(\partial\mathfrak{z}_i)(\partial\mathfrak{z}_i)}, \tag{105}$$

where the couplings $\lambda_{\mathcal{Y}\mathfrak{z}_i\mathfrak{z}_i}$ and $\lambda_{\mathcal{Y}(\partial\mathfrak{z}_i)(\partial\mathfrak{z}_i)}$ can be read off from the interaction term in the cubic action, and $K_{\mathcal{Y}\mathfrak{z}_i\mathfrak{z}_i}$ and $K_{\mathcal{Y}(\partial\mathfrak{z}_i)(\partial\mathfrak{z}_i)}$ appear in the three-point functions of the operators dual to the fields \mathfrak{z} and \mathcal{Y} ; they are functions of the conformal dimensions of these operators. From (103), we have

$$\lambda_{\mathcal{Y}\mathfrak{z}_i\mathfrak{z}_i} = -\frac{3}{2}m_i^2, \quad \lambda_{\mathcal{Y}(\partial\mathfrak{z}_i)(\partial\mathfrak{z}_i)} = 1, \tag{106}$$

$K_{\mathcal{Y}\mathfrak{z}_i\mathfrak{z}_i}$ is given by (69) and

$$K_{\mathcal{Y}(\partial\mathfrak{z}_i)(\partial\mathfrak{z}_i)} = -\frac{\Delta^2 - \Delta - 1}{\ell_2^2}K_{\mathcal{Y}\mathfrak{z}_i\mathfrak{z}_i}, \tag{107}$$

such that

$$\tilde{D}_i = -\frac{1}{\ell_2^2} \left(\frac{5}{2}\Delta(\Delta - 1) - 1 \right) K_{\mathcal{Y}\mathfrak{z}_i\mathfrak{z}_i}. \tag{108}$$

We will now report on the correction to the two-point functions due to the interaction with \mathcal{Y} for both the BPS and the non-BPS branch.

BPS branch. In the BPS branch, $\mathfrak{z} = (\varphi_i, \chi_i)$ are eigenstates of the mass matrix, and all eigenvalues of M^2 are $m^2 = \frac{2}{\ell_2^2}$. For these fields, $\Delta_{\mathfrak{z}} = 2$, such that (65) and (108) give, respectively,

$$D = \frac{6}{\pi}, \quad \tilde{D} = \frac{18}{\pi\ell_2^2}, \tag{109}$$

where we used $K_{\mathcal{Y}\mathfrak{z}_i\mathfrak{z}_i} = -9/2\pi$.

Non-BPS branch. The structure of the corrected two-point function in the non-BPS branch is similar to the one in the BPS branch, but there are important differences. The main differences come from the spectrum of conformal dimensions we have in this branch, listed in (95). We have three eigenstates with mass $m^2 = \frac{2}{\ell_2^2}$ and $\Delta = 2$; for these fields, the values of D and \tilde{D} are equivalent to those in the BPS branch in (109). For the eigenstate with mass $m^2 = \frac{6}{\ell_2^2}$ and $\Delta = 3$, one obtains

$$D = \frac{40}{3\pi}, \quad \tilde{D} = \frac{70}{\pi\ell_2^2}, \tag{110}$$

with $K_{\mathcal{Y}\mathfrak{z}_i\mathfrak{z}_i} = -5/\pi$.

However, the two eigenstates with mass $m^2 = 0$, and corresponding conformal dimension $\Delta = 1$, are more delicate. As is clear from (69), at $\Delta_{\mathfrak{z}} = 1$, the coefficient $K_{\mathcal{Y}\mathfrak{z}\mathfrak{z}}$ diverges. This divergence originates from the fact that the conformal dimensions of the operators considered sum to $\Delta_{\mathcal{Y}} + 2\Delta_{\mathfrak{z}} = d$, with $\Delta_{\mathcal{Y}} = -1$, and $d = 1$. This is a known divergence that is related to extremal correlators [54].¹¹ Since the cubic coupling in (103) is clearly not zero, we find that the corresponding \tilde{D} is divergent.

The appearance of an extremal correlator with a non-zero cubic coupling is unusual and problematic. Unusual, because in higher-dimensional theories of AdS_{d+1} —arising from a consistent truncation of a ten-dimensional compactification—the extremal cubic couplings are zero; for theories with an AdS_5 factor, see [54–56], and [57–59] for cases in AdS_3 . Problematic, because the divergence forces the conclusion that the non-BPS branch does not lead to a near- AdS_2 background with well-defined correlators.

There are two additional comments in this regard:

- Let us first consider the possibility that (103) is missing terms, and if included appropriately they should lead to a vanishing cubic coupling of the marginal operator and \mathcal{Y} . In particular, we will include h_{ab} (assuming it has a background value controlled by \mathcal{Y}). The presence of h_{ab} adds the following modification to (103) (up to overall normalisations)

$$h^{STab} \partial_a \vec{\zeta} \cdot \partial_b \vec{\zeta} - \frac{1}{2} \hat{h} \vec{\zeta}^T M^2 \vec{\zeta}. \tag{111}$$

The trace mode, \hat{h} , does not contribute for a marginal (massless) mode, and moreover, it is also decoupled from \mathcal{Y} as reflected in (43). For the symmetric traceless piece, we note that

$$\begin{aligned} h^{STab} \partial_a \vec{\zeta} \cdot \partial_b \vec{\zeta} &= \bar{\nabla}^a \bar{\nabla}^b U(x) \left(\partial_a \vec{\zeta} \cdot \partial_b \vec{\zeta} - \frac{1}{2} g_{ab} \partial_c \vec{\zeta} \cdot \partial^c \vec{\zeta} \right) \\ &= -\bar{\nabla}^b U(x) (\bar{\square} \vec{\zeta}) \cdot \partial_b \vec{\zeta} + (\text{total derivative}) \end{aligned} \tag{112}$$

which is again zero for the massless mode. This shows that the states with $\Delta = 1$ do not couple to h_{ab} and hence would not affect the cubic coupling with \mathcal{Y} even if we make h_{ab} depend on the JT field.

- In the non-BPS sector, there are other extremal correlators: cubic couplings between the moduli such that $\Delta_i = \Delta_j + \Delta_k$, which is a common occurrence since we have operators with $\Delta = 1, 2, 3$. A simple computation for our theory shows that all of these couplings λ_{ijk} are zero. This confirms that within a consistent supergravity truncation, the couplings vanish as in the higher-dimensional AdS cases.

Based on this, the conclusion we reach is that for the non-BPS branch, we have not identified correctly the near-AdS₂ background that describes the backreaction as we turn on the irrelevant deformation \mathcal{Y} . Unfortunately, it is not clear to us how to modify our definitions and setup to fix this problem while keeping the marginal operator as part of the spectrum.

5. Examples in Gauged Supergravity

In this section, we will consider some special cases in the gauged theory. In Sections 5.1 and 5.2, we are restricted to purely magnetic solutions, i.e., $Q_I = 0$ and $P^I \neq 0$, and consider two subsets of solutions to the attractor equations: non-BPS solutions following the conventions of [26], and BPS solutions described in [23,24]. We collect the attractor equations for both cases in Appendix B.1, and below discuss the non-universal properties that these backgrounds dictate at the level of the spectrum of operators and the interactions. Finally, in Section 5.3, we briefly consider a simple dyonic non-BPS example.

5.1. Magnetic Non-BPS Background

Here we will analyse a non-BPS background in the gauged theory that is supported by magnetic charges. It is a specific background that has a well-defined limit as we take $g \rightarrow 0$, and hence connects with the ungauged backgrounds. Since it is cumbersome to keep four independent charges P^I , we will further specialise to the case where $P^1 = P^2 = P^3$, and P^4 is independent; Appendices B.1 and C contain expressions when all four charges are independent.

Although we will have only two independent charges, we will see below that this example already captures interesting non-universal features. Some of these features depend on the relative sign of P^1 and P^4 ; to simplify our discussion and make the analysis more transparent, we will sometimes set $P^4 = \pm P^1$, which corresponds to the near-AdS₂ region of the magnetic RN black hole in AdS₄.

AdS₂ background. For the attractor values of the scalars, the above simplification means

$$\bar{\varphi}_1 = \bar{\varphi}_2 = \bar{\varphi}_3, \tag{113}$$

and the remaining background equations fully determine the remaining fields $\bar{\varphi}_1, \Phi_0$ and the AdS₂ radius ℓ_2 via

$$\begin{aligned} 4g^2\Phi_0^4 \sinh \bar{\varphi}_1 &= e^{\bar{\varphi}_1}(P^1)^2 - e^{-3\bar{\varphi}_1}(P^4)^2, \\ 4g^2\Phi_0^4 \cosh \bar{\varphi}_1 &= e^{\bar{\varphi}_1}(P^1)^2 + \frac{1}{3}e^{-3\bar{\varphi}_1}(P^4)^2 - \frac{4\Phi_0^2}{3}, \\ \frac{1}{\ell_2^2} &= \frac{1}{\Phi_0^2} + 6g^2 \cosh \bar{\varphi}_1. \end{aligned} \tag{114}$$

If $P^4 = \pm P^1$, the attractor equations simplify: this sets $\bar{\varphi}_1 = 0$, and (114) reduces to

$$\begin{aligned} \frac{1}{\ell_2^2} - \frac{1}{\Phi_0^2} &= 6g^2, \\ \frac{1}{\ell_2^2} + \frac{1}{\Phi_0^2} &= \frac{2(P^1)^2}{\Phi_0^4}. \end{aligned} \tag{115}$$

Spectrum of operators. Diagonalizing the mass matrix for both sectors as

$$\square \vec{\mathfrak{J}} - M^2 \vec{\mathfrak{J}} = 0, \tag{116}$$

we find its eigenvalues m^2 and corresponding orthogonal eigenstates $\vec{\mathfrak{J}} = (\mathfrak{J}_1, \dots, \mathfrak{J}_6)$ to be

$$\begin{aligned} m_1^2 = \frac{1}{\Phi_0^2} + e^{-\bar{\varphi}_1} \left(g^2 + \frac{P^1 P^4}{\Phi_0^4} \right) : & \quad \mathfrak{J}_1 = -\chi_1^{\text{hom}} + \chi_3^{\text{hom}}, \\ & \quad \mathfrak{J}_2 = -\chi_1^{\text{hom}} + 2\chi_2^{\text{hom}} - \chi_3^{\text{hom}}, \\ m_2^2 = \frac{2}{\Phi_0^2} + 4g^2 e^{-\bar{\varphi}_1} : & \quad \mathfrak{J}_3 = \varphi_1^{\text{hom}} + \varphi_2^{\text{hom}} + \varphi_3^{\text{hom}}, \\ m_3^2 = \frac{2}{\Phi_0^2} + g^2(3e^{\bar{\varphi}_1} + e^{-\bar{\varphi}_1}) : & \quad \mathfrak{J}_4 = -\varphi_1^{\text{hom}} + \varphi_3^{\text{hom}}, \\ & \quad \mathfrak{J}_5 = -\varphi_1^{\text{hom}} + 2\varphi_2^{\text{hom}} - \varphi_3^{\text{hom}}, \\ m_4^2 = \frac{2}{3\Phi_0^2} + \frac{e^{-3\bar{\varphi}_1}(P^4 - 3e^{2\bar{\varphi}_1}P^1)^2}{3\Phi_0^4} : & \quad \mathfrak{J}_6 = \chi_1^{\text{hom}} + \chi_2^{\text{hom}} + \chi_3^{\text{hom}}. \end{aligned} \tag{117}$$

If $P^4 = P^1$, there is only one degenerate mass

$$m^2 = 4g^2 + \frac{2}{\Phi_0^2} : \quad \vec{\mathfrak{J}} = (\varphi_i, \chi_i). \tag{118}$$

If $P^4 = -P^1$, we have

$$\begin{aligned} m_1^2 = -2g^2 : & \quad \mathfrak{J}_1 = -\chi_1^{\text{hom}} + \chi_3^{\text{hom}}, \\ & \quad \mathfrak{J}_2 = -\chi_1^{\text{hom}} + 2\chi_2^{\text{hom}} - \chi_3^{\text{hom}}, \\ m_{2,3}^2 = m_\varphi^2 = 4g^2 + \frac{2}{\Phi_0^2} : & \quad \mathfrak{J}_{i+2} = \varphi_i, \\ m_4^2 = \frac{2}{3} \left(\frac{4}{\ell_2^2} + \frac{5}{\Phi_0^2} \right) : & \quad \mathfrak{J}_6 = \chi_1^{\text{hom}} + \chi_2^{\text{hom}} + \chi_3^{\text{hom}}. \end{aligned} \tag{119}$$

It is instructive to inspect the conformal dimensions associated to the states (117) in more detail. Starting with the second one listed in (117), we have

$$\begin{aligned} \Delta_2 &= \frac{1}{2} + \sqrt{\frac{1}{4} + m_1^2 \ell_2^2} \\ &= \frac{1}{2} + \sqrt{\frac{9}{4} - 2g^2 \ell_2^2 e^{-\bar{\varphi}_1} - 6g^2 \ell_2^2 e^{\bar{\varphi}_1}}. \end{aligned} \tag{120}$$

It is interesting to note that the effect of the AdS₄ surrounding ($g \neq 0$) is that it lowers the conformal dimension relative to the ungauged case ($g = 0$) where the corresponding state has $\Delta_2 = 2$. From (114), the lower bound of Δ_2 is attained when $\bar{\varphi}_1 = 0$ (i.e., when $P^1 = \pm P^4$) and $6g^2 \ell_2^2 < 1$. This implies that the range of Δ_2 is

$$1.46 < \Delta_2 \leq 2, \tag{121}$$

hence making it an irrelevant operator below the JT field \mathcal{Y} . A similar analysis will show the same range of values applies for Δ_3 . For the case $P^4 = P^1$, all conformal dimensions have the range (121), and for $P^4 = -P^1$, it applies to the three eigenstates with Δ_φ .

For m_1^2 and m_4^2 , the analysis is more delicate: their final values depend on the choice of signs of P^1 and P^4 and cannot solely be determined from (114). If P^1 and P^4 have the same sign, a similar analysis will show that the ranges of Δ_1 and Δ_4 are the same as (121). In particular, this clearly holds for the case $P^4 = P^1$ given in (118). However, if P^1 and P^4 have opposite signs, we find that both bounds on Δ_4 are increased:

$$2.21 < \Delta_4 \leq 3, \tag{122}$$

such that now $\Delta_4 > \Delta_\mathcal{Y}$. For this choice of sign, the mass m_1^2 in (117) can become negative; hence, it can violate the Breitenlohner–Freedman bound. In particular, for $P^4 = -P^1$, it is clear from (119) that the mass $m_1^2 < 0$, and Δ_1 reduces to

$$\Delta_1 = \frac{1}{2} + \frac{1}{2} \sqrt{1 - 8g^2 \ell_2^2}. \tag{123}$$

Thus, when $P^1 = -P^4$, the eigenstate with mass-squared m_1^2 violates the BF bound if

$$8g^2 \ell_2^2 < 1. \tag{124}$$

This is a stricter requirement than the one implied by (115), i.e., $6g^2 \ell_2^2 < 1$. In Section 5.3, we discuss a dyonic example, $P^1 = \pm Q_1$ and the remaining charges equal to zero, for which we find the same bound (124).

Finally, notice that we can smoothly take the $g \rightarrow 0$ limit in (114) and (117). The remaining attractor equations (114) then determine the charges up to a relative sign between P^4 and P^1 . The three eigenvalues in (117) corresponding to $\mathfrak{Z}_{3,4,5}$ collapse in either case to $m^2 \ell_2^2 = 2$; for the remaining three, this depends on this relative sign. If P^1 and P^4 have the same sign, the six eigenvalues are as in the ungauged BPS case (95); if there is a relative sign, we instead land in the non-BPS case (96).

Interactions. We are now ready to discuss the interactions in the magnetic non-BPS case introduced above. The general expressions are presented in Appendix C. For clarity here we present the values for the limiting case where all magnetic charges are equal in size (i.e., we further set $P^1 = \pm P^4$).

As in Section 4.5, we will classify the corrections to the two-point functions in terms of the parameter \hat{D} defined in (73). If $P^1 = P^4$, all \hat{D}_i are equal, their value is

$$\hat{D}_i = -\frac{3}{4(\Delta_i - 1)} \left(-\frac{4}{\ell_2^2} + 16g^2 \right). \tag{125}$$

Furthermore, all conformal dimensions are equal to (120) with $\bar{\varphi}_1 = 0$. Using this in (69) to compute $K_{\mathcal{Y}3_i, 3_i}$ then determines the range of \hat{D}_i : as $0 \leq g^2 < \frac{1}{6\ell_2^2}$,

$$2.19 < \ell_2^2 \hat{D}_i \leq 3. \tag{126}$$

Thus, \hat{D}_i is always positive and setting $g = 0$ here agrees precisely with the BPS case (109), as expected.

If instead $P^1 = -P^4$, there are different behaviours since the eigenvalues do not all become degenerate. We obtain

$$\begin{aligned} \hat{D}_1 &= -\frac{3}{4(\Delta_1 - 1)} \left(\frac{1}{\ell_2^2} + g^2 \right), \\ \hat{D}_\varphi &= -\frac{3}{4(\Delta_\varphi - 1)} \left(-\frac{4}{\ell_2^2} + 16g^2 \right), \\ \hat{D}_4 &= -\frac{3}{4(\Delta_4 - 1)} \left(-\frac{14}{\ell_2^2} + 46g^2 \right). \end{aligned} \tag{127}$$

The range of \hat{D}_φ is as in (126), and for \hat{D}_4 we find

$$3.93 < \ell_2^2 \hat{D}_4 \leq \frac{21}{4}, \tag{128}$$

i.e., \hat{D}_4 is always positive as well. Setting $g = 0$ matches perfectly with the non-BPS case: \hat{D}_φ matches with (109) and \hat{D}_4 with (110). The case of \hat{D}_1 is more subtle: for $g = 0$, we get $\Delta_1 = 1$, and the correlator is extremal, and it also violates the BF bound for $g^2 > \frac{1}{8\ell_2^2}$. However, within the range $g^2 \in (0, \frac{1}{8\ell_2^2})$ \hat{D}_1 is positive.

5.2. Magnetic BPS Background

The solution in Section 5.1 is related to the BPS solution of [24], see also [23,60]. In Appendix B.1, we relate the attractor solution of [24] to the notation used in the previous section. An important point is that the BPS solution (A30) is at a very different footing as compared to the non-BPS solution (A24): all charges are proportional to g , so they are not smoothly connected to solutions in the ungauged theory.

For ease of comparison with the literature, we will adopt the conventions of [24,60] to describe the magnetic charges. Hence we will use

$$n_1 = gP^4, \quad n_2 = gP^2, \quad n_3 = gP^3, \quad n_4 = gP^1, \tag{129}$$

where n_I are integral charges.

AdS₂ background. We will again consider a subset of solutions for which three charges are equal and negative, and the remaining charge is positive. To comply with the conditions on the charges n_i given in (A27), we choose $n_2 = n_3 = n_4 < 0$ and $n_1 > 0$ such that

$$n_1 + 3n_4 = 2. \tag{130}$$

Thus, contrary to the non-BPS case, there is only one independent charge. This sets

$$\bar{\varphi}_1 = \bar{\varphi}_2 = \bar{\varphi}_3. \tag{131}$$

From (A30), the charges can be solved for as

$$n_1 = \frac{g^2 \Phi_0^2}{2} (e^{3\bar{\varphi}_1} - 3e^{\bar{\varphi}_1}), \quad n_{2,3,4} = -g^2 \Phi_0^2 \cosh \bar{\varphi}_1, \tag{132}$$

and (A31) and (A32) give

$$\frac{1}{\ell_2^2} = \frac{g^2}{4} e^{-\bar{\varphi}_1} (3 + e^{2\bar{\varphi}_1})^2, \quad \frac{1}{\Phi_0^2} = -\frac{2g^2 e^{-\bar{\varphi}_1}}{n_4 + e^{-2\bar{\varphi}_1} n_1}. \tag{133}$$

In terms of $\bar{\varphi}_1$ and Φ_0 , the constraint on the charges gives

$$\frac{1}{\Phi_0^2} = \frac{g^2}{4} e^{-\bar{\varphi}_1} \left(e^{4\bar{\varphi}_1} - 3(2e^{\bar{\varphi}_1} + 1) \right). \tag{134}$$

Spectrum of operators. At the linearised level, the inhomogeneous solution for φ_i is the same as in (A34); explicitly, for the special case we consider, we have

$$\varphi_i = \frac{2}{\Phi_0} \frac{1 - e^{2\bar{\varphi}_1}}{1 + e^{2\bar{\varphi}_1}} \mathcal{Y} + \varphi_i^{\text{hom}}, \tag{135}$$

and the inhomogeneous parts of χ_i can consistently be set to vanish. Diagonalizing the mass matrix for both sectors $(\varphi_i^{\text{hom}}, \chi_i^{\text{hom}})$ as

$$\square \vec{\mathfrak{z}} - M^2 \vec{\mathfrak{z}} = 0, \tag{136}$$

we find the mass eigenvalues and corresponding (orthogonal) eigenstates to be

$$\begin{aligned} m_1^2 = -2g^2 \sinh \bar{\varphi}_1 : & \quad \mathfrak{z}_1 = -\chi_1^{\text{hom}} + \chi_3^{\text{hom}}, \\ & \quad \mathfrak{z}_2 = -\chi_1^{\text{hom}} + 2\chi_2^{\text{hom}} - \chi_3^{\text{hom}}, \\ m_2^2 = \frac{2}{\Phi_0^2} + 4g^2 e^{-\bar{\varphi}_1} : & \quad \mathfrak{z}_3 = \varphi_1^{\text{hom}} + \varphi_2^{\text{hom}} + \varphi_3^{\text{hom}}, \\ m_3^2 = \frac{2}{\Phi_0^2} + g^2 e^{\bar{\varphi}_1} (3 + e^{-2\bar{\varphi}_1}) : & \quad \mathfrak{z}_4 = -\varphi_1^{\text{hom}} + \varphi_3^{\text{hom}}, \\ & \quad \mathfrak{z}_5 = -\varphi_1^{\text{hom}} + 2\varphi_2^{\text{hom}} - \varphi_3^{\text{hom}}, \\ m_4^2 = \frac{2}{\Phi_0^2} + 4g^2 e^{\bar{\varphi}_1} \cosh^2 \bar{\varphi}_1 : & \quad \mathfrak{z}_6 = \chi_1^{\text{hom}} + \chi_2^{\text{hom}} + \chi_3^{\text{hom}}, \end{aligned} \tag{137}$$

We can write the eigenvalues fully in terms of the charge n_4 and the gauge coupling g using (134) and

$$e^{-2\bar{\varphi}_1} = \frac{n_4}{3n_4 - 1 - \sqrt{(2n_4 - 1)(6n_4 - 1)}}. \tag{138}$$

Then it is clear that the eigenvalues are all proportional to g^2 , as expected.

Again, it is instructive to inspect the conformal dimensions associated to these eigenstates. Starting with the second listed eigenvalue, in terms of only n_4 we have

$$\Delta_2 = 2\sqrt{\frac{1 - 2n_4}{1 - 6n_4}}. \tag{139}$$

From the conditions on the charges, it is clear that $n_4 \in (-\infty, -1)$. This determines the range of Δ_2 as

$$\frac{2}{\sqrt{3}} < \Delta_2 < 2\sqrt{\frac{3}{7}}. \tag{140}$$

Similarly, we find for Δ_3

$$\Delta_3 = 1 + \sqrt{\frac{1 - 2n_4}{1 - 6n_4}}, \quad 1 + \frac{1}{\sqrt{3}} < \Delta_3 < 1 + \sqrt{\frac{3}{7}}, \tag{141}$$

and for Δ_4

$$\Delta_4 = 1 + 2\sqrt{\frac{1 - 2n_4}{1 - 6n_4}}, \quad 1 + \frac{2}{\sqrt{3}} < \Delta_4 < 1 + 2\sqrt{\frac{3}{7}}. \tag{142}$$

Thus, comparing to the irrelevant deformation \mathcal{Y} we have $1 < \Delta_2 < \Delta_3 < \Delta_{\mathcal{Y}} < \Delta_4 < 2.5$, so $\mathfrak{z}_{3,4,5}$ are less, and \mathfrak{z}_6 is more irrelevant than the JT field \mathcal{Y} . Finally, Δ_1 is given by

$$\Delta_1^\pm = \frac{1}{2} \pm \left(-\frac{1}{2} + \sqrt{\frac{1-2n_4}{1-6n_4}} \right), \tag{143}$$

where

$$\frac{1}{\sqrt{3}} < \Delta_1^+ < \sqrt{\frac{3}{7}}, \quad 1 - \sqrt{\frac{3}{7}} < \Delta_1^- < 1 - \frac{1}{\sqrt{3}}. \tag{144}$$

From (143), it is clear that the fourth mass m_4^2 takes on negative values. However, the BF bound is never violated, as both Δ_1^\pm are real for any value of the charge n_4 . The difference between $\Delta_{2,3,4}$ and Δ_1 can also be seen directly from (137). The last three eigenvalues are manifestly positive, but for the first eigenvalue, we can consider the BF bound, $m^2 + \frac{1}{4\ell_2^2} \geq 0$. With the AdS₂ radius as in (133), we find that it is never violated

$$m_1^2 + \frac{1}{4\ell_2^2} = \frac{g^2}{16} e^{-\bar{\varphi}_1} (e^{2\bar{\varphi}_1} - 5)^2 \geq 0. \tag{145}$$

Interactions. Finally, we discuss the corrections to the two-point functions of the eigenstates \mathfrak{z}_i due to cubic interactions with \mathcal{Y} . The corrections are of the form (72); the general expressions are not very insightful, so we give one explicit example:

$$\hat{D}_2 = -\frac{3}{4(\Delta_2 - 1)} \frac{g^2 e^{-\bar{\varphi}_1}}{2(1 + 3e^{2\bar{\varphi}_1})^2} \left(-9e^{8\bar{\varphi}_1} + 86e^{6\bar{\varphi}_1} + 44e^{4\bar{\varphi}_1} - 118e^{2\bar{\varphi}_1} - 3 \right), \tag{146}$$

where Δ_2 is given in (139), and we can use (138) to write this in terms of the charge n_4 only. Then $n_4 \in (-\infty, -1)$ determines

$$-19.7 g^2 < \hat{D}_2 < -4.49 g^2. \tag{147}$$

A similar calculation gives

$$\begin{aligned} 25.3 g^2 < \hat{D}_3 < 34.1 g^2, \\ 35.4 g^2 < \hat{D}_4 < 48.7 g^2, \end{aligned} \tag{148}$$

and

$$10.3 g^2 < \hat{D}_1^- < 12.4 g^2, \quad 14.1 g^2 < \hat{D}_1^+ < 23.5 g^2. \tag{149}$$

Thus, only \hat{D}_2 is negative, and all other \hat{D}_i are positive. The sign of \hat{D} is an interplay of the sign of the effective cubic coupling constant λ_{eff} of \mathcal{Y} and the field \mathfrak{z}_i , and of the conformal dimension Δ_i : the prefactor in (73) is positive for $\Delta < 1$, and negative otherwise. This is the only background for which we find a different sign for the corrections; it would be interesting to reproduce this from a near-CFT₁ description or account for it from the dual CFT₃ in the UV.

5.3. Dyonic, Non-BPS

In this section, we consider an additional example to complement the discussion in Sections 5.1 and 5.2. It is a very simple configuration: all but one field strength vanishes, and the magnetic and electric charges are matched. More concretely, here we will take $P^1 = \pm Q_1$ and all remaining charges equal to zero. This example is non-BPS, and hence we will find similar results as those described in Section 5.1. The corresponding black hole solution can be found in e.g., [26].

AdS₂ background. The attractor solution for this example is very simple. The scalars simplify to

$$\bar{\chi}_i = 0, \quad \bar{\varphi}_i = 0. \tag{150}$$

Solving the attractor equations for this background gives

$$\frac{1}{\ell_2^2} + \frac{1}{\Phi_0^2} = \frac{(Q_1)^2}{\Phi_0^4}, \quad \frac{1}{\ell_2^2} - \frac{1}{\Phi_0^2} = 6g^2. \tag{151}$$

Note that these equations imply that $\Phi_0^2 > \ell_2^2$ and $6g^2\ell_2^2 < 1$. The solution for the size of the S^2 is

$$6g^2\Phi_0^2 = -1 + \sqrt{1 + 6g^2(Q_1)^2}. \tag{152}$$

Spectrum of operators. The linearised equations (33) and (34) are also very simple. They become

$$\bar{\square}\chi_i - (4g^2 + \frac{2}{\Phi_0^2})\chi_i = 0, \tag{153}$$

and

$$\begin{aligned} \bar{\square}\varphi_1 - (4g^2 + \frac{2}{\Phi_0^2})\varphi_1 + (6g^2 + \frac{2}{\Phi_0^2})\varphi_2 + (6g^2 + \frac{2}{\Phi_0^2})\varphi_3 &= 0, \\ \bar{\square}\varphi_2 - (4g^2 + \frac{2}{\Phi_0^2})\varphi_2 - (6g^2 + \frac{2}{\Phi_0^2})\varphi_3 + (6g^2 + \frac{2}{\Phi_0^2})\varphi_1 &= 0, \\ \bar{\square}\varphi_3 - (4g^2 + \frac{2}{\Phi_0^2})\varphi_3 - (6g^2 + \frac{2}{\Phi_0^2})\varphi_2 + (6g^2 + \frac{2}{\Phi_0^2})\varphi_1 &= 0. \end{aligned} \tag{154}$$

Note that in this case, there are no terms proportional to \mathcal{Y} , and hence there are no inhomogeneous solutions ($\bar{a} = 0$).

The spectrum of conformal dimensions is the following. The masses for χ_i are easy to read off from (153), and hence we have three eigenstates $\mathfrak{z}_i, i = 3, 4, 5$ ¹² with conformal dimension

$$\begin{aligned} \Delta_\chi &= \frac{1}{2} + \sqrt{\frac{1}{4} + \ell_2^2 m_\chi^2} \\ &= \frac{1}{2} + \sqrt{\frac{9}{4} - 8\ell_2^2 g^2}. \end{aligned} \tag{155}$$

For $0 \leq 6g^2\ell_2^2 < 1$, we have $1.46 < \Delta_\chi \leq 2$ and hence the χ_i are less irrelevant than \mathcal{Y} : the effect of the AdS_4 ($g \neq 0$) surrounding is to lower the conformal dimension relative to the ungauged case. Next, diagonalizing (154), the three eigenvalues and eigenstates are

$$\begin{aligned} m_1^2 = -2g^2, \quad \Delta_1 = \frac{1}{2} + \sqrt{\frac{1}{4} - 2g^2\ell_2^2} : \quad \mathfrak{z}_1 = \varphi_1 + \varphi_3, \\ \mathfrak{z}_2 = \varphi_1 + 2\varphi_2 - \varphi_3, \\ m_2^2 = 16g^2 + \frac{6}{\Phi_0^2}, \quad \Delta_2 = \frac{1}{2} + \sqrt{\frac{25}{4} - 20g^2\ell_2^2} : \quad \mathfrak{z}_6 = -\varphi_1 + \varphi_2 + \varphi_3. \end{aligned} \tag{156}$$

Again, conformal dimensions are lowered due to the presence of g . However, more importantly, in this sector, we have two negative mass-squared states, which could trigger an instability. Demanding that m_1^2 complies with the Breitenlohner–Freedman bound in AdS_2 requires that

$$8g^2\ell_2^2 \leq 1, \quad \text{or equivalently,} \quad 2g^2\Phi_0^2 \leq 1. \tag{157}$$

In terms of the electric charge, this means

$$g^2 Q_1^2 \leq \frac{5}{2}. \tag{158}$$

Hence only black holes with very small charges (relative to the AdS₄ radius) are stable.

Interactions. Finally, we report on the corrections to the two-point functions due to a non-trivial background value of \mathcal{Y} . The corrections are of the form (72). We find

$$\begin{aligned} \Delta_\chi : \hat{D}_\chi &= -\frac{3}{4(\Delta_\chi - 1)} \left(-\frac{4}{\ell_2^2} + 16g^2 \right), \\ \Delta_1 : \hat{D}_1 &= -\frac{3}{4(\Delta_1 - 1)} \left(\frac{1}{\ell_2^2} + g^2 \right), \\ \Delta_2 : \hat{D}_2 &= -\frac{3}{4(\Delta_2 - 1)} \left(-\frac{14}{\ell_2^2} + 46g^2 \right), \end{aligned} \tag{159}$$

where \hat{D} is defined in (73). Computing them explicitly using the conformal dimensions in (155) and (156), we find that both \hat{D}_χ and \hat{D}_2 are positive for $0 \leq g^2 < \frac{1}{6\ell_2^2}$

$$\begin{aligned} 2.19 < \ell_2^2 \hat{D}_\chi &\leq 3, \\ 3.93 < \ell_2^2 \hat{D}_2 &\leq \frac{21}{4}. \end{aligned} \tag{160}$$

Again the effect of g is to lower the values relative to the ungauged theory. Setting $g = 0$ matches \hat{D}_χ with (109) and \hat{D}_2 with (110). The case \hat{D}_1 is similar to \hat{D}_1 in the magnetic non-BPS case with $P^1 = -P^4$, i.e., (127): for $g = 0$, the correlator is extremal and $K_{\mathcal{Y}_{3,4}^2}$ diverges; for $g^2 > \frac{1}{8\ell_2^2}$, the BF bound is violated. In the range $g^2 \in (0, \frac{1}{8\ell_2^2})$, \hat{D}_1 is positive.

6. Conclusions and Discussion

We explored aspects of near-AdS₂ backgrounds that appear in $\mathcal{N} = 2, D = 4$ supergravity. We focused on quantifying the spectrum of operators and their interactions with the JT sector. In Table 1, we collected the most prominent examples studied here and summarised their main features. From this table there are a few important lessons:

- *Supersymmetry is key.* In every single non-BPS example we considered, there is something undesirable: either we have unstable modes in the gauged theory, or we have problems with the extremal three-point correlators in the ungauged case. BPS backgrounds have a well-defined EFT description in all cases.
- *Gauged versus ungauged.* Not surprisingly, the effect of AdS₄, relative to Minkowski₄, on the spectrum of AdS₂ operators is to lower the conformal dimensions.¹³ This allows for the presence of operators that are relevant, or even unstable, for the gauged theory. It is one reflection of how the surrounding (UV embedding) has an imprint on the IR physics.
- *Who is relevant, marginal, and irrelevant.* It is interesting to see how the spectrum for a black hole can be plain and simple (BPS ungauged theory), or have all flavours of operators available (BPS gauged theory). This is an indication that the ingredients that go into building a statistical description of the black hole will not be universal.
- *Expected and unexpected pathologies.* One expected pathology we encountered in our analysis is the presence of modes that violate the BF bound for backgrounds in the gauged theory. This is a common occurrence in AdS₂ × ℝ² in the context of AdS/CMT [61–63], although less discussed for AdS₂ × S² [18,64]. The unexpected pathology is the non-vanishing extremal cubic coupling among the marginal operator and \mathcal{Y} for non-BPS backgrounds in the ungauged theory, as discussed in Section 4.5. Although it is well known that non-BPS black holes have a flat direction in the attractor

mechanism, it is disappointing that this spoils the construction of an effective field theory around near-AdS₂.

Table 1. A summary of our results for the different cases we considered: ungauged/gauged, BPS/non-BPS, and charge configurations. We report (the range of) the conformal dimensions, the eigenstates, and the corrections to the two-point functions as defined in (72) with \hat{D} given in (73). The ranges are for $0 \leq 6g^2\ell_2^2 < 1$. The symbol Δ^* indicates that the corresponding states can violate the BF bound if $8g^2\ell_2^2 < 1$, and that $\Delta = 1$ for $g = 0$; in those cases, we only give the sign of \hat{D} . Note that the c_i in the ungauged, non-BPS eigenstates can be read off from (97). We dropped the superscript (hom) for the magnetic gauged cases and presented the orthogonal (but not orthonormal) eigenstates for clarity and brevity.

		Spectrum		Interactions	
		(Q_I, P^I)	Δ	Eigenstates	$\langle 33 \rangle = \langle 33 \rangle_{\text{free}} (1 + \hat{D}(\dots))$
ungauged	BPS	$Q_I \neq 0,$ $P_I \neq 0$	$\Delta_3 = 2$	$\vec{3} = (\varphi_i, \chi_i)$	$\hat{D}_3 = \frac{3}{\ell_2^2}$
	non-BPS	(82), 7 independent parameters	$\Delta_1 = 1$	$\begin{cases} \vec{3}_1 = \chi_1 + \chi_3 \\ \vec{3}_2 = c_1\varphi_2 + \chi_1 + c_2\chi_2 \\ \vec{3}_3 = \varphi_1 \\ \vec{3}_4 = \varphi_3 \\ \vec{3}_5 = c_3\varphi_2 + c_4\chi_2 \end{cases}$	\hat{D}_1 undetermined
			$\Delta_2 = 2$		$\hat{D}_2 = \frac{3}{\ell_2^2}$
			$\Delta_3 = 3$		$\vec{3}_6 = c_1\varphi_2 - \chi_1 + c_2\chi_2 + \chi_3$
BPS	Magnetic, $n_1 = 2 - 3n_4$ $n_2 = n_3 = n_4$	$0.35 < \Delta_1^- < 0.42,$ $0.58 < \Delta_1^+ < 0.65$	$\begin{cases} \vec{3}_1 = -\chi_1 + \chi_3 \\ \vec{3}_2 = -\chi_1 + 2\chi_2 - \chi_3 \\ \vec{3}_3 = \varphi_1 + \varphi_2 + \varphi_3 \\ \vec{3}_4 = -\varphi_1 + \varphi_3 \\ \vec{3}_5 = -\varphi_1 + 2\varphi_2 - \varphi_3 \\ \vec{3}_6 = \chi_1 + \chi_2 + \chi_3 \end{cases}$	$10.3 g^2 < \hat{D}_1^- < 12.4 g^2,$ $14.1 g^2 < \hat{D}_1^+ < 23.5 g^2$	
		$1.15 < \Delta_2 < 1.31$		$-19.7 g^2 < \hat{D}_2 < -4.49 g^2$	
		$1.57 < \Delta_3 < 1.65$		$25.3 g^2 < \hat{D}_3 < 34.1 g^2$	
		$2.15 < \Delta_4 < 2.31$		$35.4 g^2 < \hat{D}_4 < 48.7 g^2$	
gauged	non-BPS	Magnetic, $p^1 = p^2 = p^3$ $p^4 = p^1$	$1.46 < \Delta_3 \leq 2$	$\vec{3} = (\varphi_i, \chi_i)$	$2.19 < \ell_2^2 \hat{D}_3 \leq 3$
		Magnetic, $p^1 = p^2 = p^3$ $p^4 = -p^1$	$\Delta_1^* \leq 1$ $1.46 < \Delta_\varphi \leq 2$ $2.2 < \Delta_4 \leq 3$	$\begin{cases} \vec{3}_1 = -\chi_1 + \chi_3 \\ \vec{3}_2 = -\chi_1 + 2\chi_2 - \chi_3 \end{cases}$ $\vec{3}_{i+2} = \varphi_i, \quad i = 1, 2, 3$ $\vec{3}_6 = \chi_1 + \chi_2 + \chi_3$	$\hat{D}_1 > 0$ $2.19 < \ell_2^2 \hat{D}_\varphi \leq 3$ $3.93 < \ell_2^2 \hat{D}_4 \leq \frac{21}{4}$
	BPS	Dyonic, $p^1 = \pm Q_1$ $p^{I \neq 1} = 0$ $Q_{I \neq 1} = 0$	$\Delta_1^* \leq 1$ $1.46 < \Delta_\chi \leq 2$ $2.2 < \Delta_2 \leq 3$	$\begin{cases} \vec{3}_4 = \varphi_1 + \varphi_3 \\ \vec{3}_5 = \varphi_1 + 2\varphi_2 - \varphi_3 \end{cases}$ $\vec{3}_i = \chi_i, \quad i = 1, 2, 3$ $\vec{3}_6 = -\varphi_1 + \varphi_2 + \varphi_3$	$\hat{D}_1 > 0$ $2.19 < \ell_2^2 \hat{D}_\chi \leq 3$ $3.93 < \ell_2^2 \hat{D}_2 \leq \frac{21}{4}$

Of course, here we focused on specific holographic aspects of the near-AdS₂ backgrounds: the spectrum, a specific type of interaction, and the imprint on one specific correlation function. Other interactions, other entries in the holographic dictionary and how they affect other observables would be interesting to study. A few possible future directions are the following.

6.1. From UV to IR

One of the most interesting and challenging directions to pursue is to reproduce the results of Table 1 from a dual description. This might be a feasible task for supersymmetric black holes, where we have some control already on their extremal entropy, such as the BPS black holes in the gauged and ungauged theory. For the gauged cases, it would be very interesting if one could reproduce the values of Δ from the dual CFT₃ in the UV.

In addition to the spectrum, we also reported on the cubic interactions appearing in the near-AdS₂ region and their imprint on the two-point functions. This is a non-universal entry in the holographic dictionary, and hence contains valuable information about the near-CFT₁. One direction to pursue is to connect \hat{D} to an observable outside the near-horizon region and hence tie its value and properties to a correction that can be computed in the UV description of the black hole. This should be conceptually clear, although technically cumbersome to evaluate; if feasible, it would provide a non-trivial check of our analysis.

6.2. Imprint on Quantum and Higher Derivative Corrections

A natural question is how the operator content we quantified affects the quantum entropy of black holes. In particular, we found in the gauged theory that there are matter fields with $\Delta < 3/2$, which according to [43] are the dominant effect over the Schwarzschild sector. It would be interesting to understand the connection to [65,66] and have a more refined understanding of the statistical system.

It is also important to contrast thermodynamic properties of BPS versus non-BPS black holes beyond the area law. Several issues already arose in our analysis, and it will be useful to place those in the context of quantum corrections to the black hole entropy. For example, for non-extremal black holes, the logarithmic corrections behave very differently, as illustrated in [67] versus [68]. Furthermore, the results of [65,66] show important differences between BPS and non-BPS states, which quantifies the role of the mass gap in both cases.

Finally, it would be interesting to quantify the role of higher derivative corrections in $\mathcal{N} = 2$ supergravity in our analysis. This was recently revisited for AdS₂ backgrounds for the ungauged theory in [33], and there are also some new developments in the gauged theory found by [69,70].

6.3. Black Hole Zoo

As stressed from the beginning, we only focused on backgrounds that are a direct product of AdS₂ and S²; and within the gauged theory, we considered a small subset of all solutions. It would clearly be interesting to expand this analysis and establish if the patterns found here are robust for all dyonic solutions in AdS₄.

Of course, there is also a much richer space of solutions that deserve attention. For instance, the inclusion of different horizon topologies, which is quite intricate in the gauged theory; several AdS₂ backgrounds of this form have been recently discussed in [71,72], including an overview of possible solutions in the 4D gauged theory. Rotation is also a very interesting aspect to explore, and our current work was inspired by the new features found in five-dimensional rotating black holes [5,41]. In contrast to the results in [5], we did not see a change of sign for \hat{D} for a fixed operator, which might be attributed to the lack of rotation here. Understanding and decoding the patterns in \hat{D} clearly deserves more attention. In four dimensions, rotation is a much more difficult parameter to introduce in near-AdS₂, as reflected by the analysis of near-extremal Kerr in [73]. Still, it would be interesting to understand how the interplay between rotation and supersymmetry enters in our discussion, and, in particular, to connect it with the developments in [74–76].

6.4. Integrability Conditions on Non-Extremal Black Holes

As shown in [26], which builds upon observations in [77], a generic non-extremal dyonic black hole background is not physically reasonable for $g \neq 0$ and arbitrary values of (Q_I, P^I) . In a nutshell, non-extremal AdS₄ black holes cannot carry both magnetic and

electric charge without imposing a constraint. One way to discover this inconsistency comes from demanding the integrability of the mass of the black hole. Integrable conserved charges are paramount for a well-defined phase space and the validity of the first law of thermodynamics. It would be interesting to understand how this integrability condition is present in the context of near-AdS₂. The AdS₂ background will exist for any values of (Q_I, P^I) , but there should be a restriction on how to deform away from it such that this deformation leads to an integrable non-extremal solution.

Author Contributions: The authors contributed equally to this work.

Funding: The work of AC and EV is supported in part by the Delta ITP consortium, a program of the NWO that is funded by the Dutch Ministry of Education, Culture and Science (OCW). The work of EV is part of the research programme of the Foundation for Fundamental Research on Matter (FOM), which is financially supported by NWO.

Acknowledgments: We are grateful to Alex Belin, Jan de Boer, Geoffrey Compère, Roberto Emparan, Nabil Iqbal, and Chiara Toldo for discussions on this topic.

Conflicts of Interest: The authors declare no conflict of interest. The funders had no role in the design of the study; in the collection, analyses, or interpretation of data; in the writing of the manuscript, or in the decision to publish the results.

Appendix A. Conventions

Here we gather some basic conventions used in Section 2.1 for easy comparison with other references. For a p -form ω with components defined by

$$\omega = \frac{1}{p!} \omega_{\mu_1 \dots \mu_p} dx^{\mu_1} \wedge \dots \wedge dx^{\mu_p} , \tag{A1}$$

the dual $\star\omega$ is

$$\star\omega = (\star\omega)_{\nu_1 \dots \nu_{n-p}} dx^{\nu_1} \wedge \dots \wedge dx^{\nu_{n-p}} , \tag{A2}$$

where

$$(\star\omega)_{\nu_1 \dots \nu_{n-p}} = \frac{1}{p!} \epsilon_{\nu_1 \dots \nu_{n-p} \mu_1 \dots \mu_p} \omega^{\mu_1 \dots \mu_p} . \tag{A3}$$

Here n is the number of spacetime dimensions.

The four-dimensional Levi-Civita tensor is given by

$$\epsilon_{\mu\nu\alpha\beta} = \sqrt{-g^{(4)}} \tilde{\epsilon}_{\mu\nu\alpha\beta} , \tag{A4}$$

where $\tilde{\epsilon}$ is the Levi-Civita symbol $\tilde{\epsilon}_{0123} = 1$. Furthermore, it is useful to recall that in four-dimensions, in Lorentzian signature, the top form is

$$\begin{aligned} dx^\alpha \wedge dx^\beta \wedge dx^\mu \wedge dx^\nu &= -\epsilon^{\alpha\beta\mu\nu} \sqrt{-g^{(4)}} dx^1 \wedge dx^2 \wedge dx^3 \wedge dx^4 \\ &= -\epsilon^{\alpha\beta\mu\nu} \sqrt{-g^{(4)}} d^4x . \end{aligned} \tag{A5}$$

The two-dimensional Levi-Civita tensor is given by

$$\epsilon_{ab} = \sqrt{-g^{(2)}} \tilde{\epsilon}_{ab} , \tag{A6}$$

where $\tilde{\epsilon}$ is the Levi-Civita symbol $\tilde{\epsilon}_{01} = 1$.

Appendix B. Aspects of $U(1)^4$ Supergravity

In this appendix, we collect various formulas that are used that are specific to $U(1)^4$ supergravity. In particular, we present explicit formulas related to integrating out the fields strengths in our setup. We also present the explicit attractor solutions for this theory.

We start by writing out explicitly the matrices introduced in (5). Writing h_{IJ} and k_{IJ} in matrix notation, we have

$$H \equiv -\frac{\chi_1}{2} \begin{pmatrix} 0 & 0 & 0 & 1 \\ 0 & 0 & 1 & 0 \\ 0 & 1 & 0 & 0 \\ 1 & 0 & 0 & 0 \end{pmatrix}, \tag{A7}$$

and

$$K \equiv \begin{pmatrix} k_{11} & k_{12} & k_{13} & k_{14} \\ k_{12} & k_{22} & k_{23} & k_{24} \\ k_{13} & k_{23} & k_{33} & k_{34} \\ k_{14} & k_{24} & k_{34} & k_{44} \end{pmatrix}, \tag{A8}$$

with

$$\begin{aligned} k_{11} &= e^{-\varphi_1 + \varphi_2 + \varphi_3}, \\ k_{12} &= e^{-\varphi_1 + \varphi_2 + \varphi_3} \chi_3, \\ k_{13} &= e^{-\varphi_1 + \varphi_2 + \varphi_3} \chi_2, \\ k_{14} &= -e^{-\varphi_1 + \varphi_2 + \varphi_3} \chi_2 \chi_3, \\ k_{22} &= e^{-\varphi_1 + \varphi_2 + \varphi_3} \chi_3^2 + e^{-\varphi_1 + \varphi_2 - \varphi_3}, \\ k_{23} &= e^{-\varphi_1 + \varphi_2 + \varphi_3} \chi_2 \chi_3, \\ k_{24} &= -e^{-\varphi_1 + \varphi_2 + \varphi_3} \chi_2 \chi_3^2 - e^{-\varphi_1 + \varphi_2 - \varphi_3} \chi_2, \\ k_{33} &= e^{-\varphi_1 + \varphi_2 + \varphi_3} \chi_2^2 + e^{-\varphi_1 - \varphi_2 + \varphi_3}, \\ k_{34} &= -e^{-\varphi_1 + \varphi_2 + \varphi_3} \chi_2^2 \chi_3 - e^{-\varphi_1 - \varphi_2 + \varphi_3} \chi_3, \\ k_{44} &= e^{-\varphi_1 + \varphi_2 + \varphi_3} \chi_2^2 \chi_3^2 + e^{-\varphi_1 + \varphi_2 - \varphi_3} \chi_2^2 + e^{-\varphi_1 - \varphi_2 + \varphi_3} \chi_3^2 + e^{-\varphi_1 - \varphi_2 - \varphi_3}. \end{aligned} \tag{A9}$$

A few identities that these matrices satisfy are

$$H^2 = \frac{\chi_1^2}{4} \mathbb{1}_{4 \times 4}, \tag{A10}$$

i.e., H is proportional to its own inverse, and

$$e^{-\varphi_1} H K^{-1} = e^{\varphi_1} K H. \tag{A11}$$

Using these identities, we can write the potential introduced in (19) as

$$V(\mathbf{P}, \mathbf{Q}) \equiv (\mathbf{P}^I \ \mathbf{Q}_I) \begin{pmatrix} (1 + \chi_1^2 e^{2\varphi_1}) k_{IJ} & -2e^{2\varphi_1} (kh)_I^J \\ -2e^{2\varphi_1} (hk)^I_J & (k^{-1})^{IJ} \end{pmatrix} \begin{pmatrix} \mathbf{P}^J \\ \mathbf{Q}_J \end{pmatrix}. \tag{A12}$$

When manipulating the linearised equations of motion for the scalars, it will be also useful to note that for the $U(1)^4$ theory, the potential also obeys

$$\partial_{\varphi_i}^2 V = V, \quad \partial_{\varphi_i} \partial_{\chi_i} V = \partial_{\chi_i} V, \quad \partial_{\chi_1}^2 V = 2e^{2\varphi_1} \mathbf{P}^I k_{IJ} \mathbf{P}^J. \tag{A13}$$

When solving for the equations of motion (11), the x^a components of the modified field strengths explicitly are

$$\begin{aligned}
 \mathcal{F}_{ab}^1 &= \Phi^{-3}(Q_1 + \chi_1 P^4)e^{\varphi_1 - \varphi_2 - \varphi_3}\epsilon_{ab} \\
 \tilde{\mathcal{F}}_{2ab} &= \Phi^{-3}\left(P^2 - \chi_1 Q_3 - \chi_3 Q_1 - \chi_3 \chi_1 P^4\right)e^{\varphi_1 - \varphi_2 + \varphi_3}\epsilon_{ab} \\
 \tilde{\mathcal{F}}_{3ab} &= \Phi^{-3}\left(P^3 - \chi_1 Q_2 - \chi_2 Q_1 - \chi_2 \chi_1 P^4\right)e^{\varphi_1 + \varphi_2 - \varphi_3}\epsilon_{ab} \\
 \mathcal{F}_{ab}^4 &= \Phi^{-3}\left(Q_4 - \chi_1 \chi_2 Q_3 - \chi_1 \chi_3 Q_2 - \chi_2 \chi_3 Q_1 \right. \\
 &\quad \left. - \chi_1 \chi_2 \chi_3 P^4 + \chi_3 P^3 + \chi_2 P^2 + \chi_1 P^1\right)e^{\varphi_1 + \varphi_2 + \varphi_3}\epsilon_{ab},
 \end{aligned}
 \tag{A14}$$

and we can transform them to the usual field strengths $F^I = dA^I$ and $\tilde{F}_I = d\tilde{A}_I$ via (4). The components along the 2-sphere are given explicitly in (14).

Appendix B.1. AdS₂ Backgrounds

In this section, we write more explicitly the equations that determine the AdS₂ backgrounds of Section 3.1. To start, it is useful to introduce some more notation. We will define for the magnetic charges

$$\begin{aligned}
 \mathcal{P}^1 &\equiv e^{\tilde{\varphi}_2 + \tilde{\varphi}_3}\left(P^1 - \tilde{\chi}_2 Q_3 - \tilde{\chi}_3 Q_2 - \tilde{\chi}_2 \tilde{\chi}_3 P^4\right), \\
 \mathcal{P}^2 &\equiv e^{\tilde{\varphi}_1 + \tilde{\varphi}_3}\left(P^2 - \tilde{\chi}_1 Q_3 - \tilde{\chi}_3 Q_1 - \tilde{\chi}_3 \tilde{\chi}_1 P^4\right), \\
 \mathcal{P}^3 &\equiv e^{\tilde{\varphi}_1 + \tilde{\varphi}_2}\left(P^3 - \tilde{\chi}_1 Q_2 - \tilde{\chi}_2 Q_1 - \tilde{\chi}_2 \tilde{\chi}_1 P^4\right), \\
 \mathcal{P}^4 &\equiv P_4.
 \end{aligned}
 \tag{A15}$$

For the electric charges $Q_{1,2,3}$ we have

$$Q_i \equiv e^{\tilde{\varphi}_i}\left(Q_i + \tilde{\chi}_i P^4\right),
 \tag{A16}$$

while for the fourth charge

$$Q_4 \equiv e^{\tilde{\varphi}_1 + \tilde{\varphi}_2 + \tilde{\varphi}_3}\left(Q_4 - \tilde{\chi}_1 \tilde{\chi}_2 Q_3 - \tilde{\chi}_1 \tilde{\chi}_3 Q_2 - \tilde{\chi}_2 \tilde{\chi}_3 Q_1 - \tilde{\chi}_1 \tilde{\chi}_2 \tilde{\chi}_3 P^4 + \tilde{\chi}_3 P^3 + \tilde{\chi}_2 P^2 + \tilde{\chi}_1 P^1\right).
 \tag{A17}$$

These are shifts that are completing the squares in $V(\mathbf{P}, \mathbf{Q})$, i.e., making the matrix in (A12) diagonal, and they also follow from the definitions of \mathcal{F}^I and \mathcal{F}_I in (A14).

Using Q_I and \mathcal{P}^I , the equations for φ_i in (27) reduces to

$$\begin{aligned}
 (\mathcal{P}^4)^2 - (\mathcal{P}^3)^2 - (\mathcal{P}^2)^2 + (\mathcal{P}^1)^2 - Q_1^2 + Q_2^2 + Q_3^2 - Q_4^2 + 2e^{\tilde{\varphi}_1 + \tilde{\varphi}_2 + \tilde{\varphi}_3}g^2\Phi_0^4(2\sinh \tilde{\varphi}_1 + \tilde{\chi}_1^2 e^{\tilde{\varphi}_1}) &= 0, \\
 (\mathcal{P}^4)^2 - (\mathcal{P}^3)^2 + (\mathcal{P}^2)^2 - (\mathcal{P}^1)^2 + Q_1^2 - Q_2^2 + Q_3^2 - Q_4^2 + 2e^{\tilde{\varphi}_1 + \tilde{\varphi}_2 + \tilde{\varphi}_3}g^2\Phi_0^4(2\sinh \tilde{\varphi}_2 + \tilde{\chi}_2^2 e^{\tilde{\varphi}_2}) &= 0, \\
 (\mathcal{P}^4)^2 + (\mathcal{P}^3)^2 - (\mathcal{P}^2)^2 - (\mathcal{P}^1)^2 + Q_1^2 + Q_2^2 - Q_3^2 - Q_4^2 + 2e^{\tilde{\varphi}_1 + \tilde{\varphi}_2 + \tilde{\varphi}_3}g^2\Phi_0^4(2\sinh \tilde{\varphi}_3 + \tilde{\chi}_3^2 e^{\tilde{\varphi}_3}) &= 0.
 \end{aligned}
 \tag{A18}$$

The equations for the axions (28) reduce to the following

$$\begin{aligned}
 -\mathcal{P}^4 Q_1 + \mathcal{P}^3 Q_2 + \mathcal{P}^2 Q_3 - \mathcal{P}^1 Q_4 + 2e^{\tilde{\varphi}_1 + \tilde{\varphi}_2 + \tilde{\varphi}_3}g^2\Phi_0^4\tilde{\chi}_1 &= 0, \\
 -\mathcal{P}^4 Q_2 + \mathcal{P}^3 Q_1 + \mathcal{P}^1 Q_3 - \mathcal{P}^2 Q_4 + 2e^{\tilde{\varphi}_1 + \tilde{\varphi}_2 + \tilde{\varphi}_3}g^2\Phi_0^4\tilde{\chi}_2 &= 0, \\
 -\mathcal{P}^4 Q_3 + \mathcal{P}^2 Q_1 + \mathcal{P}^1 Q_2 - \mathcal{P}^3 Q_4 + 2e^{\tilde{\varphi}_1 + \tilde{\varphi}_2 + \tilde{\varphi}_3}g^2\Phi_0^4\tilde{\chi}_3 &= 0,
 \end{aligned}
 \tag{A19}$$

The equations in (26) read in this notation

$$\begin{aligned}
 \frac{1}{\ell_2^2} &= \frac{1}{4\Phi_0^4}e^{-\tilde{\varphi}_1 - \tilde{\varphi}_2 - \tilde{\varphi}_3}\left(Q_1^2 + Q_2^2 + Q_3^2 + Q_4^2 + (\mathcal{P}^4)^2 + (\mathcal{P}^3)^2 + (\mathcal{P}^2)^2 + (\mathcal{P}^1)^2\right) \\
 &\quad + \frac{g^2}{2}\sum_i(2\cosh \tilde{\varphi}_i + \tilde{\chi}_i^2 e^{\tilde{\varphi}_i}),
 \end{aligned}
 \tag{A20}$$

and

$$\frac{1}{\Phi_0^2} = \frac{1}{4\Phi_0^4} e^{-\bar{\varphi}_1 - \bar{\varphi}_2 - \bar{\varphi}_3} \left(Q_1^2 + Q_2^2 + Q_3^2 + Q_4^2 + (\mathcal{P}^4)^2 + (\mathcal{P}^3)^2 + (\mathcal{P}^2)^2 + (\mathcal{P}^1)^2 \right) - \frac{g^2}{2} \sum_i (2 \cosh \bar{\varphi}_i + \tilde{\chi}_i^2 e^{\bar{\varphi}_i}). \tag{A21}$$

A useful linear combination is

$$\frac{1}{\ell_2^2} - \frac{1}{\Phi_0^2} = g^2 \sum_i (2 \cosh \bar{\varphi}_i + \tilde{\chi}_i^2 e^{\bar{\varphi}_i}). \tag{A22}$$

Magnetic solution, non-BPS. In the purely magnetic case, i.e., $Q_I = 0$ and $P^I \neq 0$, the attractor solution is very simple to write explicitly. All of the axions vanish at the horizon

$$\tilde{\chi}_i = 0, \tag{A23}$$

and we can solve (A18) and (A21) for the charges

$$\begin{aligned} (\mathcal{P}^1)^2 &= \Phi_0^4 \left(\frac{1}{\Phi_0^2} + g^2 (e^{-\bar{\varphi}_1} + e^{\bar{\varphi}_2} + e^{\bar{\varphi}_3}) \right) e^{\bar{\varphi}_1 + \bar{\varphi}_2 + \bar{\varphi}_3}, \\ (\mathcal{P}^2)^2 &= \Phi_0^4 \left(\frac{1}{\Phi_0^2} + g^2 (e^{\bar{\varphi}_1} + e^{-\bar{\varphi}_2} + e^{\bar{\varphi}_3}) \right) e^{\bar{\varphi}_1 + \bar{\varphi}_2 + \bar{\varphi}_3}, \\ (\mathcal{P}^3)^2 &= \Phi_0^4 \left(\frac{1}{\Phi_0^2} + g^2 (e^{\bar{\varphi}_1} + e^{\bar{\varphi}_2} + e^{-\bar{\varphi}_3}) \right) e^{\bar{\varphi}_1 + \bar{\varphi}_2 + \bar{\varphi}_3}, \\ (\mathcal{P}^4)^2 &= \Phi_0^4 \left(\frac{1}{\Phi_0^2} + g^2 (e^{-\bar{\varphi}_1} + e^{-\bar{\varphi}_2} + e^{-\bar{\varphi}_3}) \right) e^{\bar{\varphi}_1 + \bar{\varphi}_2 + \bar{\varphi}_3}, \end{aligned} \tag{A24}$$

The attractor value of the dilaton Φ_0 is given by

$$\frac{1}{\ell_2^2} = \frac{1}{\Phi_0^2} + 2g^2 \sum_i \cosh \bar{\varphi}_i. \tag{A25}$$

Magnetic solution, BPS. In Section 5.2, we discussed the BPS solution of [24], see also [23,60]. The BPS equations in the notation of [24] are¹⁴

$$\begin{aligned} 0 &= g^2 \left(L_1 + L_2 + L_3 + \frac{1}{L_1 L_2 L_3} \right) + \frac{1}{\Phi_0^2} \left(\frac{n_1}{L_1} + \frac{n_2}{L_2} + \frac{n_3}{L_3} + n_4 L_1 L_2 L_3 \right) \\ 0 &= g^2 \left(L_1 + L_2 - L_3 - \frac{1}{L_1 L_2 L_3} \right) - \frac{1}{\Phi_0^2} \left(\frac{n_1}{L_1} + \frac{n_2}{L_2} - \frac{n_3}{L_3} - n_4 L_1 L_2 L_3 \right) \\ 0 &= g^2 \left(L_1 - L_2 + L_3 - \frac{1}{L_1 L_2 L_3} \right) - \frac{1}{\Phi_0^2} \left(\frac{n_1}{L_1} - \frac{n_2}{L_2} + \frac{n_3}{L_3} - n_4 L_1 L_2 L_3 \right) \\ 0 &= g^2 \left(L_1 - L_2 - L_3 + \frac{1}{L_1 L_2 L_3} \right) - \frac{1}{\Phi_0^2} \left(\frac{n_1}{L_1} - \frac{n_2}{L_2} - \frac{n_3}{L_3} + n_4 L_1 L_2 L_3 \right) \\ \frac{4g}{\ell_2} &= g^2 \left(L_1 + L_2 + L_3 + \frac{1}{L_1 L_2 L_3} \right) - \frac{1}{\Phi_0^2} \left(\frac{n_1}{L_1} + \frac{n_2}{L_2} + \frac{n_3}{L_3} + n_4 L_1 L_2 L_3 \right) \end{aligned} \tag{A26}$$

with the additional condition that

$$\sum_I n_I = 2 \tag{A27}$$

and three of the n_I are negative. Translating to our notation, which is performed by comparing (A.2) there with (3) here, we have

$$n_1 = gP^4, \quad n_2 = gP^2, \quad n_3 = gP^3, \quad n_4 = gP^1, \tag{A28}$$

and

$$L_1 = e^{\frac{1}{2}(\varphi_1 + \varphi_2 + \varphi_3)}, \quad L_2 = e^{\frac{1}{2}(-\varphi_1 + \varphi_2 - \varphi_3)}, \quad L_3 = e^{\frac{1}{2}(-\varphi_1 - \varphi_2 + \varphi_3)}. \tag{A29}$$

Notice that (A26) are linear in the charges, while the equations of motion (A18) and (A19) are quadratic. This is expected since the BPS equations are linear conditions, while an equation of motion is non-linear. This also reflects that BPS solutions are only a subset of the attractor solutions.

It is rather easy to solve (A26) in a similar fashion as (A24): this gives

$$\begin{aligned} n_1 &= \frac{g^2 \Phi_0^2}{2} \left(-\frac{1}{L_2 L_3} + L_1^2 - L_1 L_2 - L_1 L_3 \right) \\ n_2 &= \frac{g^2 \Phi_0^2}{2} \left(-\frac{1}{L_1 L_3} + L_2^2 - L_2 L_3 - L_2 L_1 \right) \\ n_3 &= \frac{g^2 \Phi_0^2}{2} \left(-\frac{1}{L_1 L_2} + L_3^2 - L_3 L_2 - L_3 L_1 \right) \\ n_4 &= \frac{g^2 \Phi_0^2}{2} \left(\frac{1}{L_1^2 L_2^2 L_3^2} - \frac{1}{L_2 L_3} - \frac{1}{L_1 L_2} - \frac{1}{L_1 L_3} \right) \end{aligned} \tag{A30}$$

and

$$\frac{1}{\ell_2^2} = \frac{g^2}{4} \left(\frac{1 + L_1^2 L_2 L_3 + L_1 L_2^3 + L_3 + L_1 L_2 L_3^2}{L_1 L_2 L_3} \right)^2. \tag{A31}$$

A clever linear combination of (A30) also gives Φ_0 as

$$\Phi_0^2 = \frac{1}{2g^2} \left(n_4 L_1^2 L_2^2 L_3^2 - n_1 L_2 L_3 - n_2 L_1 L_3 - n_3 L_1 L_2 \right). \tag{A32}$$

The solutions (A30) solve (A18), and (A31) is just (A20). To satisfy (A21), one must further impose (A27). The condition on the negativity of three of the n_i is an extra constraint that follows from supersymmetry, i.e., the existence of a Killing spinor. From (A30), it is clear that the BPS solution given here is at a very different footing as compared to (A24): all charges are proportional to g , so they are not smoothly connected to solutions in the ungauged theory.

Appendix C. Near-AdS₂ Properties of Magnetic Backgrounds

In this appendix, we collect results regarding the magnetic backgrounds studied in Section 5. The results in this section apply for both non-BPS (Section 5.1) and BPS (Section 5.2) cases. Here, we collect aspects of the linearised equations and interactions; the attractor solutions are described in Appendix B.1. The expressions are given in the non-BPS notation; it is straightforward to translate them to the BPS language using the appropriate changes, notably (A28).

For the purely magnetic case $Q_I = 0$ and $P^I \neq 0$, the linearised equations in (33) become

$$\begin{aligned} \square \varphi_i - 2(g^2 \cosh \bar{\varphi}_j + g^2 \cosh \bar{\varphi}_k + \frac{1}{\Phi_0^2}) \varphi_i \\ + 2g^2 \sinh \bar{\varphi}_k \varphi_j + 2g^2 \sinh \bar{\varphi}_j \varphi_k + \frac{8g^2}{\Phi_0} \sinh \bar{\varphi}_i \mathcal{Y} = 0, \end{aligned} \tag{A33}$$

where $i \neq j \neq k$. We can split the solutions into homogeneous and inhomogeneous parts as in (35); the inhomogeneous parts of χ_i can consistently be set to vanish. Solving for $a_{\varphi,i}$ gives

$$\varphi_i = \frac{2}{\Phi_0} \frac{1 - e^{\bar{\varphi}_i + \bar{\varphi}_j} - e^{\bar{\varphi}_i + \bar{\varphi}_k} + e^{\bar{\varphi}_j + \bar{\varphi}_k}}{1 + e^{\bar{\varphi}_1 + \bar{\varphi}_2} + e^{\bar{\varphi}_1 + \bar{\varphi}_3} + e^{\bar{\varphi}_2 + \bar{\varphi}_3}} \mathcal{Y} + \varphi_i^{\text{hom}}. \tag{A34}$$

The homogeneous solutions $(\varphi_i^{\text{hom}}, \chi_i^{\text{hom}})$ satisfy

$$\begin{aligned} \bar{\square} \varphi_i^{\text{hom}} - 2(g^2 \cosh \bar{\varphi}_j + g^2 \cosh \bar{\varphi}_k + \frac{1}{\Phi_0^2}) \varphi_i^{\text{hom}} \\ + 2g^2 \sinh \bar{\varphi}_k \varphi_j^{\text{hom}} + 2g^2 \sinh \bar{\varphi}_j \varphi_k^{\text{hom}} = 0, \end{aligned} \tag{A35}$$

and

$$\begin{aligned} \bar{\square} \chi_i^{\text{hom}} - 2(g^2 \cosh \bar{\varphi}_j + g^2 \cosh \bar{\varphi}_k + \frac{1}{\Phi_0^2}) \chi_i^{\text{hom}} \\ - m_{ik} \chi_j^{\text{hom}} - m_{ij} \chi_k^{\text{hom}} = 0, \end{aligned} \tag{A36}$$

again with $i \neq j \neq k$, and

$$\begin{aligned} m_{12} = m_{21} &= \frac{1}{\Phi_0^4} (\mathcal{P}^1 \mathcal{P}^2 - \mathcal{P}^3 \mathcal{P}^4) e^{-\bar{\varphi}_1 - \bar{\varphi}_2 - \bar{\varphi}_3}, \\ m_{13} = m_{31} &= \frac{1}{\Phi_0^4} (\mathcal{P}^1 \mathcal{P}^3 - \mathcal{P}^2 \mathcal{P}^4) e^{-\bar{\varphi}_1 - \bar{\varphi}_2 - \bar{\varphi}_3}, \\ m_{23} = m_{32} &= \frac{1}{\Phi_0^4} (\mathcal{P}^2 \mathcal{P}^3 - \mathcal{P}^1 \mathcal{P}^4) e^{-\bar{\varphi}_1 - \bar{\varphi}_2 - \bar{\varphi}_3}. \end{aligned} \tag{A37}$$

In Sections 5.1 and 5.2, we considered a simplification in which we further set three of the charges equal, leaving only two independent charges. Explicitly, in the notation we used for the non-BPS case, we set $P^2 = P^3 = P^1$, and P^4 is independent. After making this simplification, the cubic interactions are described by the effective action

$$\begin{aligned} \mathcal{L}_{\text{int}} = \mathcal{Y} \partial_a \vec{\mathfrak{z}} \cdot \partial^a \vec{\mathfrak{z}} + a_1 \mathcal{Y} (\partial_a \mathfrak{z}_1 \partial^a \mathfrak{z}_1 + \partial_a \mathfrak{z}_2 \partial^a \mathfrak{z}_2 + \partial_a \mathfrak{z}_6 \partial^a \mathfrak{z}_6) \\ + \frac{3}{4} a_1^2 \mathfrak{z}_3 \partial^a \mathfrak{z}_3 \partial_a \mathcal{Y} - \sum_{i=1}^6 v_i \mathcal{Y} \mathfrak{z}_i \mathfrak{z}_i, \end{aligned} \tag{A38}$$

where the eigenstates in $\vec{\mathfrak{z}}$ are orthogonal and appropriately normalised. We also have

$$\vec{a} = a_1(0, 0, 1, 1, 1, 0), \quad a_1 \equiv 2 \frac{1 - e^{2\bar{\varphi}_1}}{1 + 3e^{2\bar{\varphi}_1}}, \tag{A39}$$

which parametrises the inhomogeneous terms in (A34), and the cubic coefficients are

$$\begin{aligned}
 v_1 = v_2 &= a_1 \left(\frac{(P^4)^2}{2\Phi_0^4} e^{-3\bar{\varphi}_1} - \frac{P^1 P^4}{2\Phi_0^4} e^{-\bar{\varphi}_1} + g^2 e^{-\bar{\varphi}_1} \right) \\
 &\quad + \frac{3}{2} \frac{(P^4)^2}{\Phi_0^4} e^{-3\bar{\varphi}_1} + \frac{3}{2} \frac{P^1 P^4}{\Phi_0^4} e^{-\bar{\varphi}_1} + g^2 e^{-\bar{\varphi}_1}, \\
 v_3 &= -3a_1^2 \left(\frac{(P^4)^2}{\Phi_0^4} e^{-3\bar{\varphi}_1} - g^2 e^{-\bar{\varphi}_1} \right) + 2a_1 \left(\frac{(P^4)^2}{\Phi_0^4} e^{-3\bar{\varphi}_1} + 6g^2 \sinh(\bar{\varphi}_1) \right) \\
 &\quad + 3 \frac{(P^4)^2}{\Phi_0^4} e^{-3\bar{\varphi}_1} - g^2 e^{-\bar{\varphi}_1} + 2g^2 e^{\bar{\varphi}_1}, \\
 v_4 = v_5 &= -a_1 \left(\frac{(P^1)^2}{\Phi_0^4} e^{\bar{\varphi}_1} - g^2 \sinh(\bar{\varphi}_1) \right) + 3 \frac{(P^1)^2}{\Phi_0^4} e^{\bar{\varphi}_1} + g^2 \cosh(\bar{\varphi}_1), \\
 v_6 &= a_1 \left(-\frac{9}{2} \frac{(P^1)^2}{\Phi_0^4} e^{\bar{\varphi}_1} + \frac{(P^4)^2}{2\Phi_0^4} e^{-3\bar{\varphi}_1} + \frac{P^1 P^4}{\Phi_0^4} e^{-\bar{\varphi}_1} + g^2 e^{-\bar{\varphi}_1} \right) \\
 &\quad + \frac{9}{2} \frac{(P^1)^2}{\Phi_0^4} e^{\bar{\varphi}_1} + \frac{3}{2} \frac{(P^4)^2}{\Phi_0^4} e^{-3\bar{\varphi}_1} - 3 \frac{P^1 P^4}{\Phi_0^4} e^{-\bar{\varphi}_1} + g^2 e^{-\bar{\varphi}_1}.
 \end{aligned}
 \tag{A40}$$

The ungauged theory magnetic case is recovered by setting $a_1 = 0$ (i.e., by removing the inhomogeneous solution) and $g = 0$. We stress again that these expressions apply to both BPS and non-BPS backgrounds.

In Section 5, we classify the corrections to the two-point functions of the fields \mathfrak{J}_i in terms of the parameter \hat{D} defined in (73). For the cubic interactions given in (A38), the effective coupling constants are given by

$$\begin{aligned}
 \lambda_1^{\text{eff}} = \lambda_2^{\text{eff}} &= e^{-\bar{\varphi}_1} g^2 + \frac{15}{2} e^{\bar{\varphi}_1} g^2 - 5e^{-\bar{\varphi}_1} \frac{P^1 P^4}{2\Phi_0^4} - \frac{3}{2\ell_2^2} \\
 &\quad + a_1 \left(e^{-\bar{\varphi}_1} g^2 + \frac{9}{2} e^{\bar{\varphi}_1} g^2 + e^{-\bar{\varphi}_1} \frac{P^1 P^4}{2\Phi_0^4} - \frac{1}{2\ell_2^2} \right), \\
 \lambda_3^{\text{eff}} &= 3e^{-\bar{\varphi}_1} g^2 + 13e^{\bar{\varphi}_1} g^2 - \frac{4}{\ell_2^2} + a_1 \left(6e^{-\bar{\varphi}_1} g^2 - \frac{2}{\ell_2^2} \right) - a_1^2 \left(3e^{-\bar{\varphi}_1} g^2 + 9e^{\bar{\varphi}_1} g^2 - \frac{3}{2\ell_2^2} \right), \\
 \lambda_4^{\text{eff}} = \lambda_5^{\text{eff}} &= \frac{21}{2} e^{-\bar{\varphi}_1} g^2 + \frac{11}{2} e^{\bar{\varphi}_1} g^2 - \frac{4}{\ell_2^2} - a_1 \left(3 \cosh \bar{\varphi}_1 g^2 - \frac{1}{\ell_2^2} \right), \\
 \lambda_6^{\text{eff}} &= 16e^{-\bar{\varphi}_1} g^2 + 15e^{\bar{\varphi}_1} g^2 + 5e^{-\bar{\varphi}_1} \frac{P^1 P^4}{\Phi_0^4} - \frac{9}{\ell_2^2} \\
 &\quad - a_1 \left(2e^{-\bar{\varphi}_1} g^2 - 3e^{\bar{\varphi}_1} g^2 - e^{-\bar{\varphi}_1} \frac{P^1 P^4}{\Phi_0^4} - \frac{1}{\ell_2^2} \right).
 \end{aligned}
 \tag{A41}$$

Appendix D. Near-Horizon Behaviour of Black Holes in Ungauged Theory

In Section 4.3, we discussed the eigenvectors of the linearised equations and their conformal dimensions. We showed that in the non-BPS case, the eigenvectors are linear combinations of the six scalar fields; some of them have conformal dimension $\Delta \neq 2$, and hence a different scaling near the horizon than the expected growth discussed in Section 4.4. In this appendix, we will give some details on how to take the extremal and near-horizon limits for the eigenstates in both the BPS and non-BPS branches, such that one finds the correct near-horizon response.

To define the (ungauged, static) extremal limits, we will start from the black hole solution in [19]. This solution is parametrised in terms of one mass parameter m_0 and eight charge parameters (δ_I, γ^I) . The metric is

$$ds^2 = -\frac{R(r)}{W(r)}dt^2 + \frac{W(r)}{R(r)}dr^2 + W(r)(d\theta^2 + \sin^2\theta d\phi^2), \tag{A42}$$

where $R(r)$ is a quadratic and $W^2(r)$ a quartic polynomial in r ; these functions furthermore depend on the mass parameter m_0 and charge parameters (δ_I, γ_I) . If we perform a dimensional reduction of this metric, it is clear from (7) that the dilaton is given by $\Phi(r) = \sqrt{W(r)}$. The precise definitions of $W(r)$ and $R(r)$, as well as those of the dilatons φ_i , axions χ_i , and the electric and magnetic charges (P^I, Q_I) , can be found in [19]. Relevant to the discussion here is that at extremality and in the strict near-horizon limit $r \rightarrow 0$

$$R(r) \underset{r \rightarrow 0}{=} r^2, \quad W(r) \underset{r \rightarrow 0}{=} \Phi_0^2 = \ell_2^2, \tag{A43}$$

such that we recover AdS_2 as the background metric; relative to the parametrisation in (54), we have $z = \ell_2^2/r$. For both the BPS and the non-BPS branch, the extremal limit consists of scaling

$$m_0 \sim m_0 \epsilon^2, \quad \delta_I \sim \delta_I \epsilon^0, \tag{A44}$$

with $\epsilon \rightarrow 0$. This also implies that the horizon radius $r_h \sim m_0 \epsilon^2 \rightarrow 0$. The scaling of the γ_I determines in which branch we land. We summarise the different possibilities in Table A1.

Table A1. Different possible extremal limits, up to permutations. The second column contains its relation to solutions of the attractor equations in Appendix B.1 for $g = 0$. In the non-BPS case, the solutions are more complex and depend on the detailed configuration.

Extremal Limit	Attractor Solution
$e^{\gamma_I} \sim e^{\gamma_I} \epsilon^{-1}$ or $e^{\gamma_I} \sim e^{\gamma_I} \epsilon$	BPS: $\mathcal{P}^1 = \mathcal{P}^2 = \mathcal{P}^3 = \mathcal{P}^4, Q_1 = Q_2 = Q_3 = Q_4$
$e^{\gamma_{1,2}} \sim e^{\gamma_{1,2}} \epsilon^{-1}$ & $e^{\gamma_{3,4}} \sim e^{\gamma_{3,4}} \epsilon$	BPS: $\mathcal{P}^1 = \mathcal{P}^2 = -\mathcal{P}^3 = -\mathcal{P}^4, Q_1 = Q_2 = -Q_3 = -Q_4$
$e^{\gamma_1} \sim e^{\gamma_1} \epsilon^{-1}$ & $e^{\gamma_{i \neq 1}} \sim e^{\gamma_{i \neq 1}} \epsilon$	non-BPS
$e^{\gamma_1} \sim e^{\gamma_1} \epsilon^{-1}$ & $e^{\gamma_{i \neq 1}} \sim e^{\gamma_{i \neq 1}} \epsilon^0$	non-BPS

For the BPS branch, the choice of an extremal limit also determines the number of relative minus signs. For both extremal limits that give the non-BPS branch, it is possible to tune the δ_I in such a way that one gets all or some of the \mathcal{P}^I and Q_I charges equal (up to minus signs). An easy example for the second non-BPS extremal limit in Table A1 is

$$\delta_1 = \delta_2 = \delta_3 \Rightarrow \mathcal{P}^1 = -\mathcal{P}^2 = -\mathcal{P}^3 = -\mathcal{P}^4, Q_1 = Q_2 = Q_3 = -Q_4, \tag{A45}$$

where $\delta_3 \neq 0$. These conditions on δ_I do not impose that any of the physical charges \mathcal{P}^I and Q_I are equal. Note, however, that from this example, it is clear that this non-BPS limit does not include the purely magnetic case (for which all $\delta_I = 0$). In general, both non-BPS limits assume that the charge parameters (δ_I, γ_I) are finite; for special cases where (some of) the charges vanish, one should first impose that before taking an extremal limit.¹⁵ Finally, by choosing different numerical values for the δ_I and γ_I , one will end up in a non-BPS solution that does not comply with (80); it can be checked numerically that the eigenvalues are still as in (96).

In Section 4.4, we discussed the linear response of the dilaton and axion fields away from their attractor values. At extremality ($\epsilon = 0$), the horizon radius is at $r_h = 0$, and we can expand the scalar fields around it to find in the BPS branch (for any extremal limit)

$$\begin{aligned} \varphi_i &= \bar{\varphi}_i + \varphi_i^{(1)} r + \dots, \\ \chi_i &= \bar{\chi}_i + \chi_i^{(1)} r + \dots, \end{aligned} \tag{A46}$$

as predicted by the nAttractor mechanism [16]. For a general non-BPS solution, this will still be true. However, for the non-BPS case, the single scalar fields are generally not eigenstates of the linearised equations of motion. Considering the near-horizon expansion of the eigenstates instead, we find again a linear response for the eigenvectors with $m^2 = \frac{2}{\ell_2^2}$, but for the eigenvectors with $m^2 = 0$ or $m^2 = \frac{6}{\ell_2^2}$ we find that the linear term cancels exactly. For some special cases that comply with (80), this will already happen at the level of the dilatons and axions: for example, for the case discussed around (97), the linear terms of χ_1 and χ_3 vanish (as could have been expected from the eigenvector \mathfrak{z}_1).

To illustrate this cancellation, let us consider the following numerical example for the first non-BPS limit in Table A1

$$e^{\delta_1} = \frac{1}{2}, e^{\delta_2} = 3, e^{\delta_3} = 5, e^{\delta_4} = 7, e^{\gamma_1} = 11\epsilon^{-1}, e^{\gamma_2} = 13, e^{\gamma_3} = \frac{1}{11}, e^{\gamma_4} = 19. \tag{A47}$$

The eigenstates of the mass matrix are

$$\begin{aligned} m^2 \ell_2^2 = 0 : \quad & \mathfrak{z}_1 = -0.1826 \varphi_1 + 0.928779 \varphi_3 + 1.35251 \chi_1 + \chi_3, \\ & \mathfrak{z}_2 = -0.133794 \varphi_1 + 1.26839 \cdot 10^{-5} \varphi_2 + 0.991009 \chi_1 + \chi_2, \\ m^2 \ell_2^2 = 2 : \quad & \mathfrak{z}_3 = 7.40696 \varphi_1 + \chi_1, \\ & \mathfrak{z}_4 = -7.88398 \cdot 10^4 \varphi_2 + \chi_2, \\ & \mathfrak{z}_5 = -1.07668 \varphi_3 + \chi_3, \\ m^2 \ell_2^2 = 6 : \quad & \mathfrak{z}_6 = 0.1826 \varphi_1 + 1.73108 \cdot 10^{-5} \varphi_2 + 0.928779 \varphi_3 \\ & \quad - 1.35251 \chi_1 + 1.36478 \chi_2 + \chi_3, \end{aligned} \tag{A48}$$

This is what our analysis predicts for the eigenstates. On the other hand, if we take the corresponding on-shell solution in [19] with these same charges, and upon taking the near-horizon limit $r \rightarrow 0$, the moduli all have linear responses

$$\begin{aligned} \chi_1 &= \bar{\chi}_{1,0} - 0.122629 r + O(r^2) & \varphi_1 &= \bar{\varphi}_{1,0} - 2.30464 r + O(r^2) \\ \chi_2 &= \bar{\chi}_{2,0} - 3.1277 \cdot 10^{-7} r + O(r^2) & \varphi_2 &= \bar{\varphi}_{2,0} + 5.59775 r + O(r^2) \\ \chi_3 &= \bar{\chi}_{3,0} + 8.49969 r + O(r^2) & \varphi_3 &= \bar{\varphi}_{3,0} - 1.70457 r + O(r^2) \end{aligned} \tag{A49}$$

but if we consider the near-horizon linear combinations dictated by the eigenvectors (A48) we find

$$\begin{aligned} m^2 \ell_2^2 = 0 : \quad & \mathfrak{z}_1 = -2.23152 + O(r^2), \quad \mathfrak{z}_2 = 6332.26 + O(r^2), \\ m^2 \ell_2^2 = 2 : \quad & \mathfrak{z}_3 = 6.18617 - 17.3815 r + O(r^2), \quad \mathfrak{z}_4 = -784443 - 441326 r + O(r^2), \\ & \mathfrak{z}_5 = 2.26974 + 3.42844 r + O(r^2), \\ m^2 \ell_2^2 = 6 : \quad & \mathfrak{z}_6 = 8643.32 + O(r^2), \end{aligned} \tag{A50}$$

Thus, indeed, the eigenvectors with $m^2 \ell_2^2 = 2$ still have a linear response, as predicted, but for the eigenvectors with $m^2 \ell_2^2 = \{0, 6\}$ this linear term vanishes in accordance with (99).

It is also worth mentioning that the non-BPS eigenstates with $m^2 \ell_2^2 = \{0, 6\}$ are easily overlooked in simple cases. For example, in the purely magnetic or purely electric non-BPS case, the eigenvectors are

$$\begin{aligned} m^2 \ell_2^2 = 0 : \quad & \mathfrak{z}_1 = \chi_1 + \chi_2, \quad \mathfrak{z}_2 = \chi_1 + \chi_3, \\ m^2 \ell_2^2 = 2 : \quad & \mathfrak{z}_3 = \varphi_1, \quad \mathfrak{z}_4 = \varphi_2, \quad \mathfrak{z}_5 = \varphi_3, \\ m^2 \ell_2^2 = 6 : \quad & \mathfrak{z}_6 = -\chi_1 + \chi_2 + \chi_3, \end{aligned} \tag{A51}$$

but for these cases, the axions actually vanish for the corresponding black hole, such that we are left only with the eigenvectors φ_i , which have the usual linear response.

Notes

- 1 BPS stands for saturation of the Bogomolnyi-Prasad-Sommerfield bound, which here we use to denote that the solution preserves a fraction of supersymmetry. Non-BPS denotes that the solution preserves no supersymmetry.
- 2 At extremality, a recent analysis of $\text{AdS}_2 \times S^2$ solutions of $\mathcal{N} = 2$ ungauged supergravity viewed from the perspective of the 2D gravity can be found in [33], which includes higher derivative corrections. An excellent review, using the technology of the quantum entropy function, is presented in [34].
- 3 In the following, x will be a shorthand referring to the two-dimensional coordinates x^a , and not the four-dimensional coordinates x^μ . For example, $\Phi(x) \equiv \Phi(x^a)$.
- 4 Our definition of P^I and Q_I is exactly the same as in [26], and they are presented in geometrical units. Other suitable ways to normalise the charges are $\bar{P}^I = \frac{P^I}{4G_4}$ and $\bar{Q}_I = \frac{Q_I}{4G_4}$, or to introduce quantised charges as $p^I = \frac{P^I}{\sqrt{4G_4}}$ and $q_I = \frac{Q_I}{\sqrt{4G_4}}$.
- 5 $V(\mathbf{P}, \mathbf{Q})$ has several simplifications and identities that apply for the $U(1)^4$ theory. These are listed in Appendix B.
- 6 About notation: ψ_i are the components of $\vec{\psi}$, and explicitly we have $(\psi_1, \psi_2, \psi_3, \psi_4, \psi_5, \psi_6) = (\varphi_1, \varphi_2, \varphi_3, \chi_1, \chi_2, \chi_3)$.
- 7 The addition of Φ_0^{-1} in (61) is to make the field \mathcal{Y} dimensionless.
- 8 Despite appearances, (80) does not imply that the physical charges (Q_I, P^I) are set equal: on the BPS branch, these conditions allow for 4 electric and 4 magnetic independent charges. For solutions on the non-BPS branch that comply with (80), there will be at least one constraint among (Q_I, P^I) , and hence this type of solution is not the most general non-BPS configuration.
- 9 This also agrees with the lowest modes in the spectrum of fluctuations of the scalar moduli in [50–52].
- 10 A straightforward check can be done with, for example, the solutions in [23,24,26].
- 11 In an extremal three-point function, the conformal dimension of one of the operators is equal to the sum of the remaining ones, e.g., $\Delta_1 = \Delta_2 + \Delta_3$. For the evaluation of (70), the irrelevant deformation \mathcal{Y} is in the Δ_- branch, such that we have $d = \Delta_- + \Delta_2 + \Delta_3$ which is the same statement.
- 12 The labelling of eigenstates is such that the conformal dimensions increase as we go from \mathfrak{z}_1 to \mathfrak{z}_6 .
- 13 This also happens in AdS_5 ; see [41].
- 14 In these equations, we restored the gauge coupling g^2 . Note that the coupling in [24] differs from the one used here by a factor $\sqrt{2}$.
- 15 In doing so, one will find that neither non-BPS limit in Table A1 accommodates the purely electric case $\gamma_I = 0$. To get this, one has to switch the scalings of δ_I and γ_I of the first non-BPS limit: take all $\gamma_I \sim \epsilon^0$ and impose the suitable scalings on δ_I .

References

1. Almheiri, A.; Polchinski, J. Models of AdS_2 backreaction and holography. *JHEP* **2015**, *11*, 014. [\[CrossRef\]](#)
2. Maldacena, J.; Stanford, D.; Yang, Z. Conformal symmetry and its breaking in two dimensional Nearly Anti-de-Sitter space. *PTEP* **2016**, *2016*, 12C104. [\[CrossRef\]](#)
3. Jackiw, R. Lower Dimensional Gravity. *Nucl. Phys.* **1985**, *B252*, 343–356. [\[CrossRef\]](#)
4. Teitelboim, C. Gravitation and Hamiltonian Structure in Two Space-Time Dimensions. *Phys. Lett.* **1983**, *126B*, 41–45. [\[CrossRef\]](#)
5. Castro, A.; Pedraza, J.F.; Toldo, C.; Verheijden, E. Rotating 5D Black Holes: Interactions and deformations near extremality. *arXiv* **2021**, arXiv:2106.00649.
6. Narayan, K. Aspects of two-dimensional dilaton gravity, dimensional reduction, and holography. *Phys. Rev. D* **2021**, *104*, 026007. [\[CrossRef\]](#)
7. Ferrara, S.; Kallosh, R.; Strominger, A. N=2 extremal black holes. *Phys. Rev.* **1995**, *D52*, 5412–5416. [\[CrossRef\]](#)
8. Strominger, A. Macroscopic Entropy of $N = 2$ Extremal Black Holes. *Phys. Lett.* **1996**, *B383*, 39–43. [\[CrossRef\]](#)
9. Ferrara, S.; Kallosh, R. Supersymmetry and Attractors. *Phys. Rev.* **1996**, *D54*, 1514–1524. [\[CrossRef\]](#)
10. Ferrara, S.; Gibbons, G.W.; Kallosh, R. Black holes and critical points in moduli space. *Nucl. Phys. B* **1997**, *500*, 75–93. [\[CrossRef\]](#)
11. Goldstein, K.; Iizuka, N.; Jena, R.P.; Trivedi, S.P. Non-supersymmetric attractors. *Phys. Rev.* **2005**, *D72*, 124021. [\[CrossRef\]](#)
12. Alishahiha, M.; Ebrahim, H. Non-supersymmetric attractors and entropy function. *JHEP* **2006**, *3*, 003. [\[CrossRef\]](#)
13. Kallosh, R.; Sivanandam, N.; Soroush, M. The Non-BPS black hole attractor equation. *JHEP* **2006**, *3*, 060. [\[CrossRef\]](#)
14. Ceresole, A.; Dall’Agata, G. Flow Equations for Non-BPS Extremal Black Holes. *JHEP* **2007**, *3*, 110. [\[CrossRef\]](#)
15. Tripathy, P.K.; Trivedi, S.P. Non-Supersymmetric Attractors in String Theory. *JHEP* **2006**, *3*, 022. [\[CrossRef\]](#)
16. Larsen, F. A nAttractor mechanism for nAdS₂/nCFT₁ holography. *JHEP* **2019**, *4*, 055. [\[CrossRef\]](#)
17. Breitenlohner, P.; Freedman, D.Z. Positive Energy in anti-De Sitter Backgrounds and Gauged Extended Supergravity. *Phys. Lett. B* **1982**, *115*, 197–201. [\[CrossRef\]](#)
18. Gubser, S.S. Breaking an Abelian gauge symmetry near a black hole horizon. *Phys. Rev. D* **2008**, *78*, 065034. [\[CrossRef\]](#)
19. Chow, D.D.K.; Compère, G. Black holes in N=8 supergravity from SO(4,4) hidden symmetries. *Phys. Rev.* **2014**, *D90*, 025029. [\[CrossRef\]](#)
20. Cvetic, M.; Pope, C.N.; Saha, A. Conformal Symmetries for Extremal Black Holes with General Asymptotic Scalars in STU Supergravity. *arXiv* **2021**, arXiv:2102.02826.
21. Gimon, E.G.; Larsen, F.; Simon, J. Black holes in Supergravity: The Non-BPS branch. *JHEP* **2008**, *1*, 040. [\[CrossRef\]](#)

22. Bellucci, S.; Ferrara, S.; Marrani, A.; Yeranyan, A. stu Black Holes Unveiled. *Entropy* **2008**, *10*, 507. [[CrossRef](#)]
23. Cacciatori, S.L.; Klemm, D. Supersymmetric AdS(4) black holes and attractors. *JHEP* **2010**, *1*, 085. [[CrossRef](#)]
24. Benini, F.; Hristov, K.; Zaffaroni, A. Black hole microstates in AdS₄ from supersymmetric localization. *JHEP* **2016**, *5*, 054. [[CrossRef](#)]
25. Cvetič, M.; Duff, M.J.; Hoxha, P.; Liu, J.T.; Lu, H.; Lu, J.X.; Martinez-Acosta, R.; Pope, C.N.; Sati, H.; Tran, T.A. Embedding AdS black holes in ten-dimensions and eleven-dimensions. *Nucl. Phys. B* **1999**, *558*, 96–126. [[CrossRef](#)]
26. Chow, D.D.K.; Compère, G. Dyonic AdS black holes in maximal gauged supergravity. *Phys. Rev. D* **2014**, *89*, 065003. [[CrossRef](#)]
27. Katmadas, S. Static BPS black holes in U(1) gauged supergravity. *JHEP* **2014**, *9*, 027. [[CrossRef](#)]
28. Halmagyi, N. Static BPS black holes in AdS₄ with general dyonic charges. *JHEP* **2015**, *3*, 032. [[CrossRef](#)]
29. Benini, F.; Hristov, K.; Zaffaroni, A. Exact microstate counting for dyonic black holes in AdS₄. *Phys. Lett.* **2017**, *B771*, 462–466. [[CrossRef](#)]
30. Gnechchi, A.; Toldo, C. On the non-BPS first order flow in N=2 U(1)-gauged Supergravity. *JHEP* **2013**, *3*, 088. [[CrossRef](#)]
31. Almheiri, A.; Kang, B. Conformal Symmetry Breaking and Thermodynamics of Near-Extremal Black Holes. *JHEP* **2016**, *10*, 052. [[CrossRef](#)]
32. Nayak, P.; Shukla, A.; Soni, R.M.; Trivedi, S.P.; Vishal, V. On the Dynamics of Near-Extremal Black Holes. *JHEP* **2018**, *9*, 048. [[CrossRef](#)]
33. Aniceto, P.; Lopes Cardoso, G.; Nampuri, S. R² corrected AdS₂ holography. *JHEP* **2021**, *3*, 255. [[CrossRef](#)]
34. Sen, A. Black Hole Entropy Function and the Attractor Mechanism in Higher Derivative Gravity. *JHEP* **2005**, *9*, 038. [[CrossRef](#)]
35. Gross, D.J.; Rosenhaus, V. A Generalization of Sachdev-Ye-Kitaev. *JHEP* **2017**, *2*, 093. [[CrossRef](#)]
36. Anninos, D.; Galante, D.A. Constructing AdS₂ flow geometries. *JHEP* **2021**, *2*, 045. [[CrossRef](#)]
37. Fu, W.; Gaiotto, D.; Maldacena, J.; Sachdev, S. Supersymmetric Sachdev-Ye-Kitaev models. *Phys. Rev. D* **2017**, *95*, 026009; Erratum in **2017**, *95*, 069904. [[CrossRef](#)]
38. Murugan, J.; Stanford, D.; Witten, E. More on Supersymmetric and 2d Analogs of the SYK Model. *JHEP* **2017**, *8*, 146. [[CrossRef](#)]
39. Marcus, E.; Vandoren, S. A new class of SYK-like models with maximal chaos. *JHEP* **2019**, *1*, 166. [[CrossRef](#)]
40. Chong, Z.W.; Cvetič, M.; Lu, H.; Pope, C.N. Charged rotating black holes in four-dimensional gauged and ungauged supergravities. *Nucl. Phys. B* **2005**, *717*, 246–271. [[CrossRef](#)]
41. Castro, A.; Larsen, F.; Papadimitriou, I. 5D rotating black holes and the nAdS₂/nCFT₁ correspondence. *JHEP* **2018**, *10*, 042. [[CrossRef](#)]
42. Michelson, J.; Spradlin, M. Supergravity spectrum on AdS(2) × S². *JHEP* **1999**, *9*, 029. [[CrossRef](#)]
43. Maldacena, J.; Stanford, D. Remarks on the Sachdev-Ye-Kitaev model. *Phys. Rev. D* **2016**, *94*, 106002. [[CrossRef](#)]
44. Larsen, F.; Lisboa, P. Quantum Corrections to Supergravity on AdS₂ × S². *Phys. Rev.* **2015**, *D91*, 084056. [[CrossRef](#)]
45. Larsen, F.; Zeng, Y. Black hole spectroscopy and AdS₂ holography. *JHEP* **2019**, *4*, 164. [[CrossRef](#)]
46. Freedman, D.Z.; Mathur, S.D.; Matusis, A.; Rastelli, L. Correlation functions in the CFT(d)/AdS(d+1) correspondence. *Nucl. Phys. B* **1999**, *546*, 96–118. [[CrossRef](#)]
47. Kallosh, R.; Kol, B. E(7) symmetric area of the black hole horizon. *Phys. Rev. D* **1996**, *53*, R5344–R5348. [[CrossRef](#)]
48. Duff, M.J. String triality, black hole entropy and Cayley’s hyperdeterminant. *Phys. Rev. D* **2007**, *76*, 025017. [[CrossRef](#)]
49. Itzhaki, N. D6 + D0 and five-dimensional spinning black hole. *JHEP* **1998**, *9*, 018. [[CrossRef](#)]
50. Banerjee, S.; Gupta, R.K.; Mandal, I.; Sen, A. Logarithmic Corrections to N=4 and N=8 Black Hole Entropy: A One Loop Test of Quantum Gravity. *JHEP* **2011**, *11*, 143. [[CrossRef](#)]
51. Sen, A. Logarithmic Corrections to N=2 Black Hole Entropy: An Infrared Window into the Microstates. *Gen. Rel. Grav.* **2012**, *44*, 1207–1266. [[CrossRef](#)]
52. Keeler, C.; Larsen, F.; Lisboa, P. Logarithmic Corrections to N ≥ 2 Black Hole Entropy. *Phys. Rev.* **2014**, *D90*, 043011. [[CrossRef](#)]
53. Nampuri, S.; Tripathy, P.K.; Trivedi, S.P. On The Stability of Non-Supersymmetric Attractors in String Theory. *JHEP* **2007**, *8*, 054. [[CrossRef](#)]
54. D’Hoker, E.; Freedman, D.Z.; Mathur, S.D.; Matusis, A.; Rastelli, L. Extremal correlators in the AdS/CFT correspondence. In *The Many Faces Of The Superworld: Yuri Golfand Memorial*; World Scientific: Singapore, 1999; pp. 332–360. [[CrossRef](#)]
55. Lee, S.; Minwalla, S.; Rangamani, M.; Seiberg, N. Three point functions of chiral operators in D = 4, N=4 SYM at large N. *Adv. Theor. Math. Phys.* **1998**, *2*, 697–718. [[CrossRef](#)]
56. Liu, H.; Tseytlin, A.A. Dilaton—Fixed scalar correlators and AdS(5) × S⁵—SYM correspondence. *JHEP* **1999**, *10*, 003. [[CrossRef](#)]
57. Mihailescu, M. Correlation functions for chiral primaries in D = 6 supergravity on AdS(3) × S³. *JHEP* **2000**, *2*, 007. [[CrossRef](#)]
58. Arutyunov, G.; Pankiewicz, A.; Theisen, S. Cubic couplings in D = 6 N=4b supergravity on AdS(3) × S³. *Phys. Rev. D* **2001**, *63*, 044024. [[CrossRef](#)]
59. Taylor, M. Matching of correlators in AdS(3) / CFT(2). *JHEP* **2008**, *6*, 010. [[CrossRef](#)]
60. Hristov, K.; Vandoren, S. Static supersymmetric black holes in AdS₄ with spherical symmetry. *JHEP* **2011**, *4*, 047. [[CrossRef](#)]
61. Denef, F.; Hartnoll, S.A. Landscape of superconducting membranes. *Phys. Rev. D* **2009**, *79*, 126008. [[CrossRef](#)]
62. Iqbal, N.; Liu, H.; Mezei, M. Lectures on holographic non-Fermi liquids and quantum phase transitions. *String Theory Its Appl.* **2012**. [[CrossRef](#)]
63. Hartnoll, S.A.; Lucas, A.; Sachdev, S. Holographic quantum matter. *arXiv* **2016**, arXiv:1612.07324.
64. Sonner, J. A Rotating Holographic Superconductor. *Phys. Rev. D* **2009**, *80*, 084031. [[CrossRef](#)]

-
65. Heydeman, M.; Iliesiu, L.V.; Turiaci, G.J.; Zhao, W. The statistical mechanics of near-BPS black holes. *J. Phys. A Math. Theor.* **2021**. [[CrossRef](#)]
 66. Iliesiu, L.V.; Turiaci, G.J. The statistical mechanics of near-extremal black holes. *JHEP* **2021**, *5*, 145. [[CrossRef](#)]
 67. Charles, A.M.; Larsen, F. Universal corrections to non-extremal black hole entropy in $\mathcal{N} \geq 2$ supergravity. *JHEP* **2015**, *6*, 200. [[CrossRef](#)]
 68. Castro, A.; Godet, V.; Larsen, F.; Zeng, Y. Logarithmic Corrections to Black Hole Entropy: The Non-BPS Branch. *JHEP* **2018**, *5*, 079. [[CrossRef](#)]
 69. Bobev, N.; Charles, A.M.; Hristov, K.; Reys, V. Higher-derivative supergravity, AdS₄ holography, and black holes. *JHEP* **2021**, *8*, 173. [[CrossRef](#)]
 70. Genolini, P.B.; Richmond, P. Supersymmetry of higher-derivative supergravity in AdS₄ holography. *Phys. Rev. D* **2021**, *104*, L061902. [[CrossRef](#)]
 71. Ferrero, P.; Inglese, M.; Martelli, D.; Sparks, J. Multi-charge accelerating black holes and spinning spindles. *arXiv* **2021**, arXiv:2109.14625.
 72. Couzens, C.; Stemerdink, K.; van de Heisteeg, D. M2-branes on Discs and Multi-Charged Spindles. *arXiv* **2021**, arXiv:2110.00571.
 73. Castro, A.; Godet, V.; Simón, J.; Song, W.; Yu, B. Gravitational perturbations from NHEK to Kerr. *JHEP* **2021**, *7*, 218. [[CrossRef](#)]
 74. Anninos, D.; Anous, T.; D'Agnolo, R.T. Marginal deformations & rotating horizons. *JHEP* **2017**, *12*, 095. [[CrossRef](#)]
 75. Larsen, F.; Paranjape, S. Thermodynamics of Near BPS Black Holes in AdS₄ and AdS₇. *J. High Energy Phys.* **2021**, *2021*, 1–44. [[CrossRef](#)]
 76. David, M.; Nian, J. Universal entropy and hawking radiation of near-extremal AdS₄ black holes. *JHEP* **2021**, *4*, 256. [[CrossRef](#)]
 77. Lü, H.; Pang, Y.; Pope, C.N. AdS Dyon Black Hole and its Thermodynamics. *JHEP* **2013**, *11*, 033. [[CrossRef](#)]